Piezoelectric Fibers: Processing and Challenges

Sarah Scheffler, Philippe Poulin

Piezoelectric fibers: processing and challenges

*Sarah Scheffler, Philippe Poulin**

AUTHOR ADDRESS : Centre de recherche Paul Pascal, CNRS, Pessac, 33600, France

KEYWORDS: piezoelectric – fiber - smart textiles – process – fiber spinning – fiber extrusion –- composites

Graphical abstract:

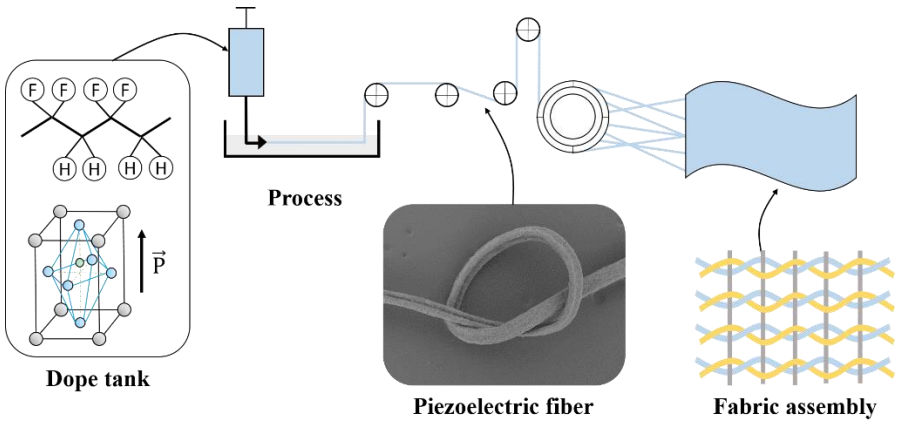

Abstract

Integration of piezoelectric materials in composite and textile structures is promising to create smart textiles with sensing or energy harvesting functionalities. The most direct integration that combines wearability, comfort and piezoelectric efficiency consists in using fibers made of piezoelectric materials. The latter include inorganic ceramics or organic polymers. Ceramics have outstanding piezoelectric properties but can not be easily melted or solubilized in a solvent to be processed in the form of fibers. They have to be spun from precursor materials and thermally treated afterwards for densification and sintering. These delicate processes have to be carefully controlled to optimize the piezoelectric properties of the fibers. On the other hand, organic piezoelectric polymers, such as Polyvinylidene fluoride (PVDF), can be spun by more

conventional textile fibers technologies. In addition to enjoy an easier manufacturing, organic piezoelectric fibers display flexibility that facilitates their integration and use in smart textiles. However, organic fibers suffer from a low piezoelectric efficiency.

This article reviews the processing techniques and their specific limitations and advantages to realize single component or coaxial piezofibers. Fundamental challenges related to the use of composite fibers are discussed. The latter include challenges for poling and electrically wiring the fibers to collect charges under operation, or to apply electrical fields. The electromechanical properties of these fibers processed by different manufacturing techniques are compared. Recent studies of structures used to integrate such fibers in textiles and composites with conventional techniques and their potential applications are discussed.

Introduction

Piezoelectric materials convert mechanical energy into electrical energy and conversely.[1] The generation of electrical charges in response to a mechanical stress, also called direct piezoelectric effect, is the basis of a variety of commercially available force sensors, strain gauges, microphones, lighters, etc. In recent years, novel applications for robotics,[2–4] tactile sensors,[5,6] internet of things (IoT),[7,8] microelectromechanical systems (MEMS),[9–11] energy harvesting[12–15] to power micro devices and wearable electronics[16] have attracted an increasing interest in the field. Energy harvesting is indeed becoming a critical challenge associated to the development of autonomous sensor networks.[17] Piezoelectric energy harvesting is based on the conversion of ambient mechanical vibrations into electrical energy. Considering its apparent simplicity and versatility, this concept is considered as one of the most promising approach among energy harvesting technologies.[13,18–20] Vibrations and mechanical energy are ubiquitous. They can be generated by industrial engines, vehicles, home appliances, body motion, or environmental sources such as rain and wind. Be it of industrial, biological or natural origin, a small fraction of this energy could generally be sufficient to power wearable electronic devices.

On the other hand, piezoelectric materials can convert electrical energy into mechanical energy. They deform in response to an applied voltage. This reverse piezoelectric effect is used in micro-actuators, ultrasonic generators, nanopositioning systems, acousto-optic modulators, active vibration damping, etc.[2,4,21–24]

Piezoelectricity arises in non-centrosymmetric atomic structures. Inorganic materials with perovskite structures such as $PbZr_xTi_{1-x}O_3$ (PZT)[25,26] and $BaTiO_3$[27] are among the most popular ones. These materials display high piezoelectric coefficients d_{33} and d_{31}.[1] These coefficients

reflect the amount of charges generated in response to an applied stress. The efficiency of inorganic materials is also manifested by high coupling coefficients, *k*, that represent the ratio of electrical to mechanical energy conversion.[1] Some organic materials, and in particular fluorinated polymers,[21,28–32] also display piezoelectric properties. The most efficient ones include polyvinylidene fluoride (PVDF) and copolymers[32,33] such as poly(vinylidenefluoride-trifluoroethylene) (PVDF-TrFE)), poly(vinylidenefluoride-trifluoroethylene-chlorotrifluoroethylene) (PVDF-TrFE-CFE) or poly(vinylidene fluoride-hexafluoropropylene (PVDF-HFP).

Organic or inorganic materials are often used under the form of thin films or small crystals. However, their applications could be extended and optimized if the materials could be used under other macroscopic forms. The form of fiber is particularly appealing for several reasons. Because of their small diameter, fibers are flexible and can be implemented in a wealth of structures, from clothing to composite materials through bags, belts, curtains, biomedical equipment and smart textiles in general.[7,34] Second, the performances and properties of materials are generally enhanced when they are processed in the form of fibers. In the world of inorganic materials, glass and carbon fibers are broadly used in composites for their excellent mechanical properties.[35,36] Record performances of organic polymers are achieved in synthetic fibers which can be drawn and highly aligned.[37,38] Small diameter fibers also enjoy a lower probability of having large defects and display therefore a greater strength to failure compared to macroscopic films.[37,39] The above advantages explain the fast increasing interest in piezoelectric fibers.

However, even if particularly appealing, the development of piezoelectric fibers and textiles remains a technical and scientific challenge. The synthesis of inorganic fibers is particularly challenging because these materials can not be melted or dissolved in common solvents. Inorganic fibers are processed from precursor materials made of mixtures of particles

and polymers or by sol-gel approaches followed by delicate thermal treatments.[40,41] Organic fibers can be more easily processed by conventional polymer fiber spinning technologies.[42,43] The mechanical properties and piezoelectric performances of the fibers can substantially vary depending on their composition and processing. Last, their implementation in actual applications is also raising technical difficulties. Fibers, such as other piezoelectric materials, have indeed to be electrically wired and mechanically fixed so that their electromechanical properties can be exploited.[34,44] Electrical wiring is necessary for the polarization of the fibers, for their electrical stimulation when used as actuators, or for the collection of electrical charges when they are deformed. In spite of these difficulties, exciting progresses have been achieved in the last years towards the synthesis of efficient and promising piezoelectric fibers.

These fibers can be implemented in smart textiles and composite materials. Their applications and performances have been reviewed in excellent recent articles.[45–47] Instead, the present review focusses on their processing and challenges for their efficient use. Typical fibers for these applications have diameters in between 1 and 100 μm. Fibers of smaller diameters, called nanofibers, made for example by electrospinning, are not considered. Piezoelectric nanowires and mats of electrospun nanofibers[6,29,48,49] are interesting materials that can be used in energy harvesting and nanogenerator applications.[50,51] However, they are not meant for long fiber reinforced composites or composition of smart fabrics. This is why nanowires, nanofibers and nanogenerators are not detailed in the present article. Interested readers can find more information in excellent recent review articles.[45,51–56] On the other hand, large cylindrical structures are also interesting because they allow an easy implementation in co-axial structures.[57,58] But, with a diameter well above 100 μm, they suffer from a high flexural stiffness and are not suitable for being the base of textiles or composite materials.

The review is divided in four sections. After this introduction, the first section presents the main approaches for the realization of inorganic piezoelectric fibers. The second section

focusses on organic polymer fibers. Advantages and drawbacks of these different materials are discussed. More recent and promising composite fibers are presented in the third section. We discuss the critical features to make this more recent approach technically viable and efficient. The fourth section briefly recalls some applications and challenges for the implementation of piezoelectric fibers in actual applications. We discuss in particular smart textiles applications, and also applications of so-called Active Fiber Composites (AFC) which are materials made of inorganic piezoelectric fibers embedded in polymeric matrices. Directions towards further progress in the field and prospects are summarized in the conclusion.

1 . Inorganic piezoelectric fibers

1.1 Piezoceramic fibers

Inorganic piezoceramics display excellent piezoelectric properties, with piezoelectric coefficients generally much greater than that of organic materials.[59,60] Some inorganic materials have piezoelectric coefficients up to 650 pC/N.[59] The major drawback of these materials is that they are brittle, especially in the fiber form. Processing conditions have a strong impact on the morphology at the macro and micro scales and are therefore critical for optimization of mechanical properties. Post-synthesis treatments are also important to control the final chemical composition of the fibers and their homogeneity. Electronic microscopy is generally used to have a qualitative idea of the porosity of a fiber. For more quantitative analysis, researchers typically calculate the apparent density and compare it with the theoretical value. The apparent density is calculated by measuring the volume and weight of several fibers. The general objective is the achievement of low porosity fibers that are sufficiently strong and flexible to be easily manipulated and implemented in applications. Because of its high piezoelectric performances, PZT has been by far the material most studied in this field.

1.1.1. Ceramic fibers process

There are three main methods to make piezoceramic fibers: the thermoplastic extrusion, the viscous solution spinning process (VSSP) and the sol-gel extrusion. As detailed below, the first two methods are more versatile in terms of chemical composition because inorganic compounds, otherwise not spinnable, are mixed with polymer materials that play the role of a matrix system of the spun fibers. In the last method, there is no need of additional components to form a matrix, but the inorganic precursors have to be directly spinnable.

1.1.1.1. Thermoplastic extrusion

In this process, a powder containing piezoelectric inorganic micro or nanoparticles is directly mixed with a thermoplastic polymer. The blend is then extruded above,[61,62] or just below[63] the melting temperature of the polymer, as in conventional melt spinning of polymer fibers,[64–66]. The obtained green fibers, which are as-spun fibers, are then heated to remove the polymer, and the inorganic grains are then sintered. Typical morphology of the final fiber can be seen in Figure 1. The key challenge of this method is to have a high loading of inorganic solid content and to keep a sufficiently low viscosity of the melt so that fibers can be extruded. In addition, the final fibers should present low porosity, high density and no macroscopic defects to have the best electromechanical performances. Grain size over 1 µm is generally used to reduce grain boundary interfaces, porosity and promote a high electromechanical coupling. Thermoplastic extrusion has already been developed to an industrial scale. CeraNova for example produces PZT fibers on large scale.[67,68] This company used a mix containing up to 60%vol of PZT-5A. This process enables the final fiber to have a diameter from 80 µm to 160 µm.

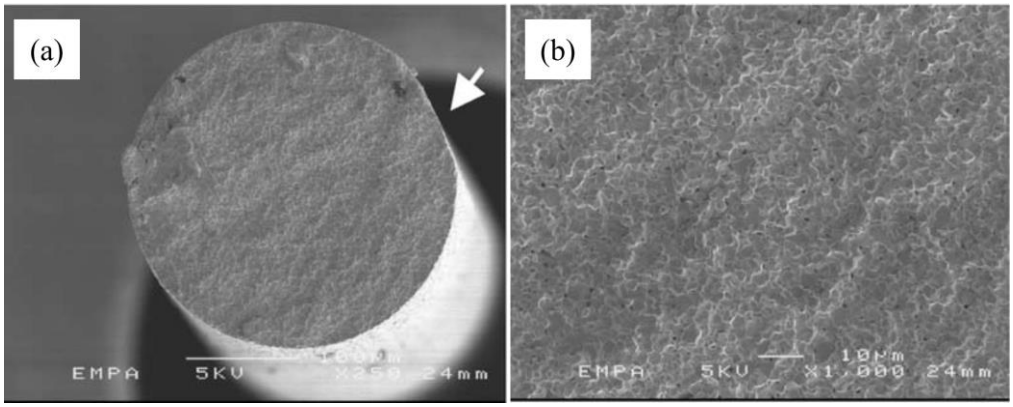

Figure 1. SEM picture of commercial PZT-5A fibers made by thermoplastic extrusion process. a) cross section and b) Magnification of the cross section. Taken from[69] with permission.

The thermoplastic polymer plays of course a key role on the viscosity of the blend, especially with grain size over 1 µm. With such a grain size and using ethylene-vinyl acetate

copolymer resin and surfactant, Sebastian *et al.*[63] were not able to extrude the green PZT fiber loaded at 60%vol, even with a large die of 500 µm. Bowen *et al.*[70] succeeded in extruding a blend of polyvinyl butyral and PZT without surfactant, through a die of approximately 250 µm. In this process, a low porosity of approximately 1 %[70] was achievable.

A good dispersion is critical to extrude the blend and have a small fiber diameter. Aggregates can indeed cause fiber rupture or clogging of the spinneret dies. Heiber *et al.*[61] studied the effect of the blending composition and of its preparation. They showed that the addition of stearic acid to a mix of polyethylene and 58%vol PZT lowers the viscosity of the blend. In addition to facilitate extrusion, this approach prevents from the formation of particle aggregates. The authors succeeded in extruding and drawing green fibers of 90 µm in diameter.

1.1.1.2. Viscous solution spinning (VSSP)

In this approach, the piezoelectric powder is mixed with a spinnable polymer solution. The green fibers are then formed by a solution spinning process, as opposed to a melt spinning process. The polymer coagulates in a non-solvent medium to form a composite fiber in which inorganic particles are trapped. The starting solution can be made of viscose (cellulose xanthane dissolved in caustic soda). The blend of piezoceramic and viscose are spun into a coagulation bath of sulphuric acid and sodium sulfate. Zinc salt can be added in order to reduce the coagulation rate and have a better control over the fiber formation and flexibility. The organic binder is removed afterwards, and densification of the fiber is performed by a sintering treatment at high temperature. The obtained fibers can have a diameter from 10 µm to more than 200 µm.[71,72] A related technique based on cellulose has been patented and was called the Alceru (ALternative CElluose Rudolstadt) process, which is a modified Lyocell manufacturing method.[73] This process has been developed at the industrial level by Advanced Cerametrics Inc. and Smart Material Corp. for respectively viscose and Alceru fibers.[74]The major advantage of the VSSP and the thermoplastic extrusion processes is their versatility via the creation of a

green precursor fiber. Because the polymer is not removed at this stage, the green fibers can be easily manipulated. After being implemented in the desired forms, the polymer can be removed by a thermal treatment and the inorganic material sintered. However, care must be taken in order to avoid fusion of the fibers during the sintering process.

1.1.1.3. Sol-gel extrusion

Piezoceramic fibers can also be formed with an alkoxide based sol-gel process in acidic conditions.[75] First, a sol is synthesised with the required amount of precursors. The spinnability of this sol is ensured by controlling its viscosity, hydrolysis and condensation rates. The sol has to be cured a certain time to reach the desired viscosity. This curing time should not be too long because the sol may form non-spinnable gel with time. Having a long spinnability time, which is the time before gelation, is an important challenge for large-scale production.[76] The liquid sol is extruded through a spinneret and the formed gel fibers are dried and collected on a take-up drum. The amorphous fibers are finally crystallised and sintered at temperatures up to 1200°C[77] or treated by microwaves.[78] Crystallisation of the PZT perovskite phase starts at 530-550°C[75,76] however, several authors[77,79] claimed that temperatures over 1000°C are needed in order to completely suppress the pyrochlore phase and to make high density fibers.The method is delicate but enjoys several advantages, including a perfect control of the chemical composition, a good homogeneity with few structural defects and a large range of accessible fiber diameters, typically from 20 to 300 µm.[75,76,79] An example of the final morphology of the fiber can be seen in Figure 2. In the case of PZT, acetic acid is added to increase the fiber drawing time.[80] Qiu *et al*.[76] studied the effect of acetic acid on the spinnability of a PZT sol. Adding the right amount of acid, and curing at 80°C for 600 min, leads to a sol of a long spinnability time. Extrusion was also facilitated by addition of PZT powder. The authors claimed that this blending promotes densification of the fibers.

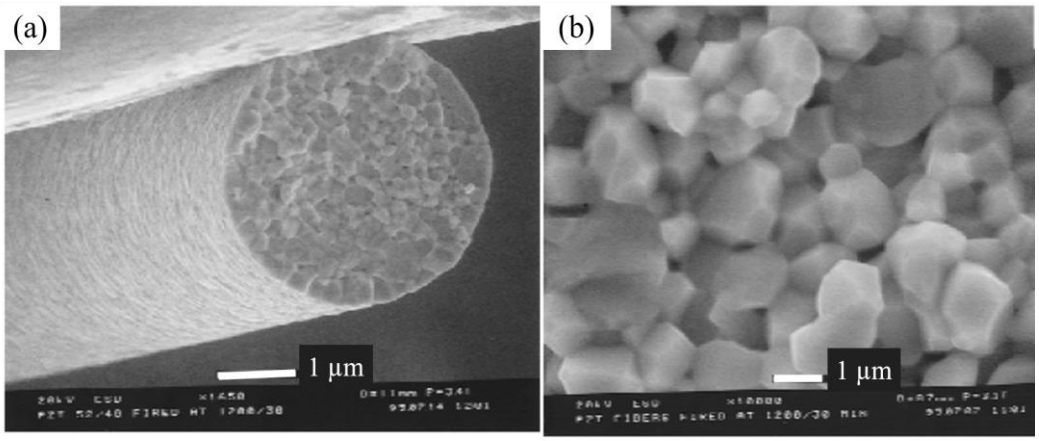

Figure 2. SEM picture of PZT fibers formed by the sol-gel process after a thermal treatment at 1200°C. a) fiber cross section, b) magnification of the fracture. The scale bar is 1 µm. Taken from[80] with permission.

The three methods described above can all provide long fiber production. Dent *et al.*[81] compared PZT fibers formed by different techniques provided by industrial suppliers. Surprisingly, the fibers formed by the sol-gel process presented the lowest density and the highest porosity of 16 vol%. Kornmann *et al.*[69] as well compared industrial fibers and measured their Young's modulus. All the results were close with a Young's modulus of about 40 GPa. This value is slightly below 50 GPa, the Young's modulus of bulk PZT. The VSSP method is slow and technically difficult but enjoys a great versatility and can be used to make small diameter fibers. The thermoplastic extrusion extrusion is a simple and robust process that allows a variety of inorganic materials to be shaped under the form of fibers. However, it suffers from the need of finely controlling the viscosity of the polymer blend by limiting the amount of inorganic particles. The limited amount of inorganic particles makes debinding and densification more difficult. The sintering operation has to be carefully performed to achieve the desired chemical composition and porosity. The sol-gel process is more appropriate to achieve a well-defined chemical composition. However, the major drawback is the difficulty to

find the right rate of hydrolysis in order to have a long time of spinnability. In all cases, ceramic fibers are brittle and can essentially be used in the form composite materials. Piezoelectric fibers aligned and embedded in a polymer matrix, named ActiveFiber Composite (AFC), are typically used for applications.[82–85]

1.1.2. Piezoelectric properties of ceramic fibers

Two methods are generally employed to measure the piezoelectric properties of ceramic fibers. Single fiber measurements, can be undertaken by applying electrical connection on both ends of the fiber, if it is large enough to be handled. Another method to measure electromechanical properties is the use of AFC. Ceramic fibers are aligned and embedded into a soft matrix, typically composed of epoxy resin.[70] To polarise ceramic fibers, contact poling is used with an electric field above 10 kV/cm for several minutes.

1.1.2.1. Active fiber composites

Measuring the piezoelectric properties at the level of individual fibers is challenging because of their brittleness. Another, more accessible, method consists in measuring properties at the level of AFC systems (Figure 3a). In such a structure, fibers can be poled perpendicular or parallel to their long axis as shown in Figure 3b. Their piezoelectric properties can be exploited and measured in different modes. However, high electric fields must be used to perform poling. Indeed, the permittivity of the ceramic fibers is much higher than the one of the polymer matrix. The electric field seen by the fiber is then much lower than the one applied. Application of high electric fields necessitates a good adhesion between the fibers and the matrix to avoid electrical breakdown due to morphological defects. A good adhesion is also needed to ensure an efficient mechanical stress transfer. The realization of AFCs is probably today the most efficient and most common way to implement piezoelectric fibers in numerous applications. Nevertheless, as discussed below, AFC materials are stiff and rigid structures. They are not suitable to exploit piezoelectric fibers as textile or cable structures.

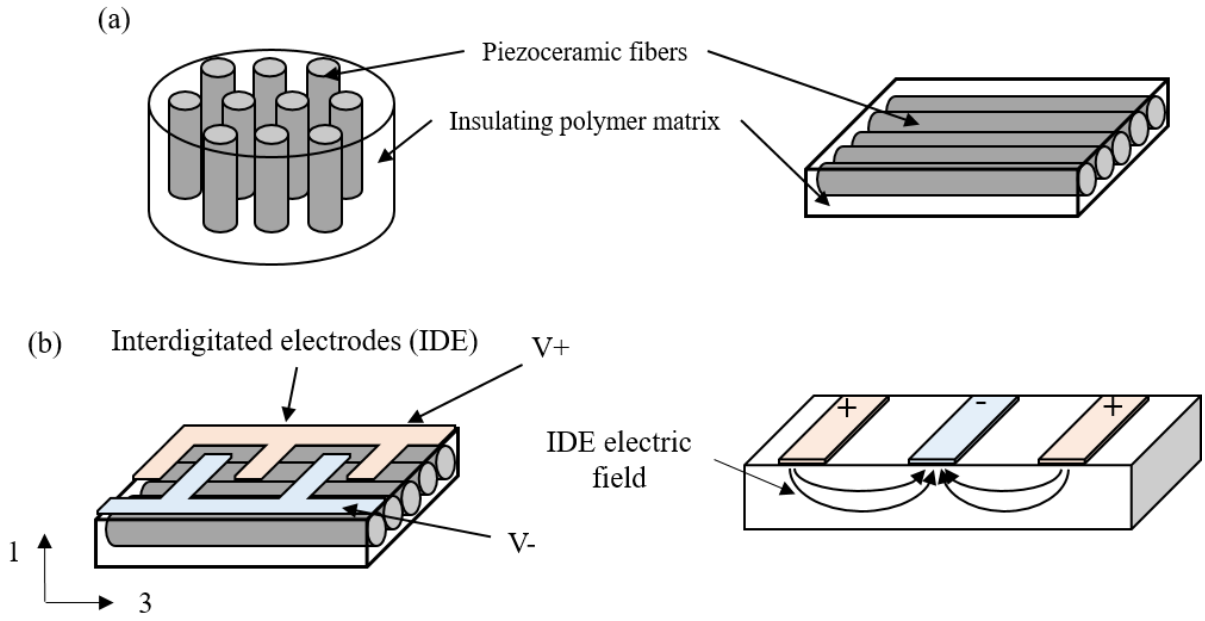

Figure 3. a) Scheme of AFC with active piezoelectric fibers in a passive polymer matrix. b) Schemes of AFC with interdigitated electrodes. The fibers are poled in the direction of their long axis so that the measured piezoelectric coefficient is the d_{33} coefficient.

The link between the piezoelectric properties of AFCs at a macroscopic level and the piezoelectric properties of individual fibers requires some modelling. For this purpose, the effective homogeneous medium model[77] is generally employed. This analytical model[78] is based on three main assumptions: (i) the lateral spatial scale of the composite is sufficiently fine for the forces applied to be effectively transferred to the ceramic fibers (ii) the piezoelectric response of the material is linear (iii) there is a perfect stress transfer between the fiber and the

matrix. Knowing the volume fraction of the fibers, the relationships[76] between the AFC composites and of the fibers, are

$$d_{33}^{composite} = d_{33}^{fiber} \frac{\upsilon s_{11}}{\upsilon s_{11} + (1-\upsilon) s_{33}^{E}}$$

$$k_{33}^{composite} = d_{33}^{composite} (\varepsilon_{33}^{T} s_{33}^{E})^{-0.5}$$

with υ the fiber volume fraction, d_{33} the piezoelectric coefficient, s_{11} and s_{33}^{E} the compliance of the fiber and the matrix (at constant field) respectively. k_{33} is the coupling coefficient and ε_{33}^{T} is the permittivity at constant strain of the composite. These equations are based on simple rules of mixture. A high amount of fibers in the composite is required to reach good piezoelectric properties. According to Nelson *et al.*[76], the d_{33} coefficient of the composite can be lower than the one of the bulk but the k_{33} coefficient can yet be high because of the mechanical properties of the soft matrix. However, a volume fraction of 20% is needed to reach the maximum piezoelectric coefficient. This is in agreement with the study of Mohammadi *et al.*[72] They studied the effect of the PZT fiber diameter and AFC thickness on the electromechanical properties of the composites. According to them, with the same volume fraction of 40%vol of fibers, the d_{33} coefficient remained almost constant at a given AFC thickness for all fiber diameter and increased linearly with the AFC thickness.

1.1.2.2. Piezoelectric properties

Piezoelectricity is characterized by several parameters. Table 1 summarizes the values of these parameters from different studies. The morphology of the fiber (grain size and diameter), the technique used to measure the piezoelectric coefficient, the coupling coefficient (k), d_{33} coefficient and the maximum strain are presented.

Table 1. Summary of piezoelectric properties of ceramic fibers. The measured values of the bulk are in bold.

Powder	Process	Diameter (µm)	Grains size (µm)	Measure	k	d_{33} (pC/N)	Maximum strain (%)	ref
PZT	sol-gel	10 to 30	2.1	AFC (70%vol)	0.53			[73]
PZT	sol-gel	10 and 50		AFC (<25%vol)	0.53	127 - **270**		[74]
PZT	sol-gel	250	2 - 6	AFC			0.17 - **0.18**	[76]
PZT	thermoplastic extrusion	260		single fiber		284	0.45	[63]
PZT-EC65	VSSP	15		AFC (40%vol)	0.55	320		[72]
PZT-5A	Thermoplastic extrusion	130		AFC		235		[78]
PZT - 5A	Thermoplastic extrusion	130		AFC	0.60 - **0.70**	278 - **374**		[76]
PZT - 5A	Sol-gel	125 and 250		AFC	0.70 and 0.61 - **0.70**	315 and 263 - **374**		[76]
PZT - 5A	VSSP	235		AFC	0.69 **(0.70**	295 - **374**		[76]
PZT-5A	Thermoplastic extrusion	233	2.5	AFC	0.73 - **0.7**	377 - **374**		[70]
PLZT	Thermoplastic extrusion	300	7.12	single fiber		443 - **410**	0.63 - **0.48**	[92]
BTO	sol-gel	20		single fiber		172		[78]
BTO	Thermoplastic extrusion	320		single fiber		72	0.063	[63]
KNL-NTS	thermoplastic extrusion	400	1.30	Single fiber		139	0.13	[93]

The piezoelectric coefficients of ceramic fibers are lower than the coefficients of the bulk material but still remain on the same order of magnitude. It appears that comparable properties can be achieved using different processes, the main factors being the chemical composition, density and porosity.

1.2. Coaxial piezoceramic fibers

The brittleness of piezoceramic fibers and the difficulty of poling them efficiently with external electrodes in AFCs have motivated the development of more complex structures. Indeed, the electrical field seen by the fibers in AFCs is lower than the field applied macroscopically because of the mismatch of permittivity between the fibers and the matrix. Among these more complex structures, coaxial fibers are gaining a strong interest. The core of coaxial fibers is made of a metal or carbon material. In addition to playing the role of electrode, the core material mechanically reinforces the fiber. The presence of a conductive core electrode allows the fibers to be poled radially, with the field perpendicular to the main fiber axis. The fiber used under tension or compression therefore operates in d_{31} mode. The d_{31} coefficient of piezoceramics is generally lower than the d_{33} coefficient.[59,94] For PZT materials, the d_{31} coefficient is approximately twice lower than the d_{33} coefficient. Nevertheless, this lower efficiency could be largely compensated by a more effective polarisation.

Coaxial fibers display some particular features. Because of their specific geometry, the applied field for poling is greater at the inner wall of the fiber than at the outer wall. A low aspect ratio of the coaxial fiber leads to a higher difference of the electric field on the inner and outer wall, and can affect the polarisation (Figure 4a). In addition, the piezoelectric efficiency depends naturally on the amount of active materials in a composite but also on the aspect ratio $\alpha = \frac{t}{r_0}$ with t the thickness of the piezoelectric layer and r_0 the total fiber diameter.[95,96] Ones need to consider the difference between the fiber density and the volume fraction when working

with coaxial fibers. With a high aspect ratio, AFC can have a high fiber density (ie a high number of fibers) but a low volume fraction of the active phase (Figure 4b).

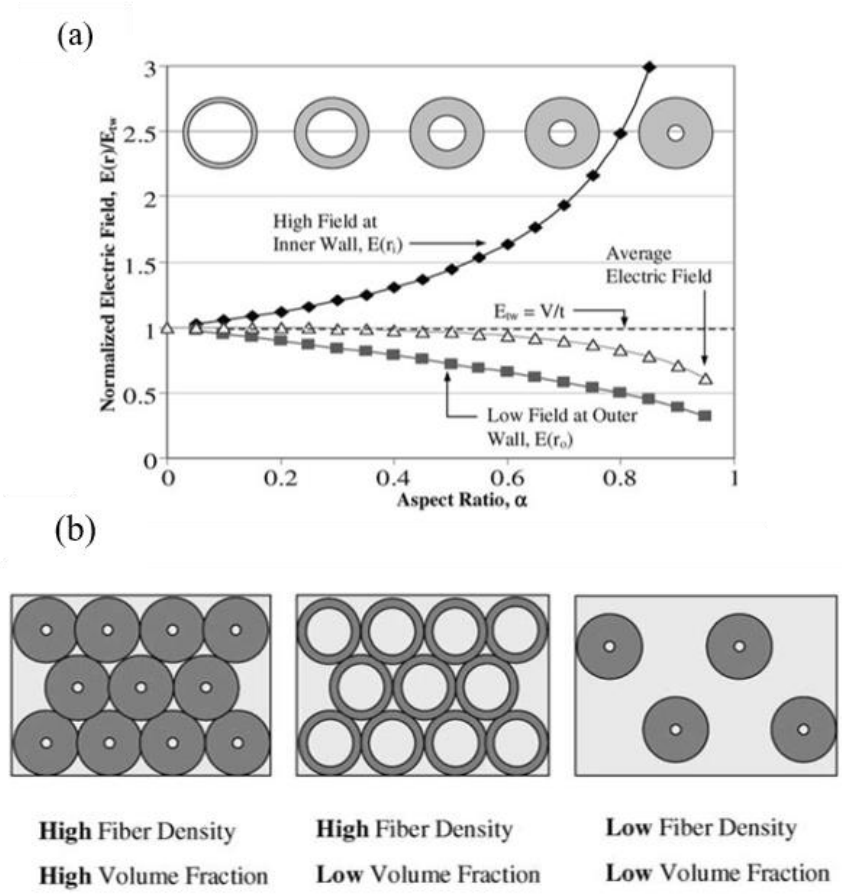

Figure 4. a) Electric field at different positions within a hollow fiber versus the aspect ratio. Increase of the aspect ratio enhances the difference of the electric field between the inner and outer walls. b) Schematic representation of AFCs with different volume fraction and fiber density. The volume fraction refers to the volume occupied by the ceramic. The fiber density is the number of fibers inside the composite. Taken from[95] with permission.

When used in a composite and as modelled in the literature,[95,96] the ratio of Young's moduli of the fiber and of the matrix material has also be taken into account. Modelling predicts that the effective d_{31} coefficient increases with the volume fraction and density of the fibers.[95,96] The effective d_{31} coefficient decreases with increasing the Young's modulus of the matrix (Figure 5). An optimal aspect ratio α is predicted for achieving the greatest effective d_{31}. This

optimal α depends on the ratio of Young's moduli.[95,96] Considering the above expectations, the control of the synthesis of coaxial piezoelectric fibers is critical to rationally optimize their use in composite applications.

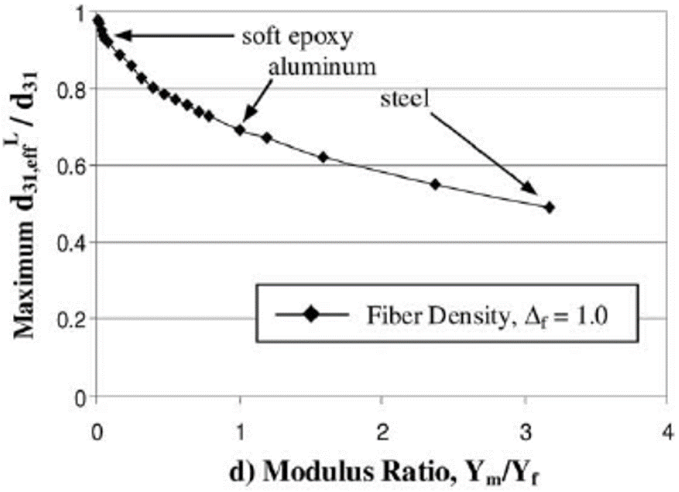

Figure 5. The calculated value of normalised d_{31} coefficient of the AFC versus the ratio of the Young modulus of the matrix and of the fiber. Soft epoxy matrix appears as the best choice in order to have the maximum effective d_{31}. Taken from[95] with permission.

1.2.1. Synthesis of coaxial piezoelectric inorganic fibers

1.2.1.1. Coextrusion

The coextrusion process is based on the thermoplastic extrusion, as described in section 1.1.1.1. In addition to this processing technique, a conductive fiber core is guided through a cylinder, as schematized in Figure 6a. This extrusion is followed by debinding and sintering treatments. Typically, fibers of more than 200 µm in diameter can be formed by this technique.[97,98] The metallic core and the green fiber have to be extruded at the same linear speed to avoid the formation of cracks, and to keep the inner fiber well centered.[98] An other technique consist in drilling a hole in an extruded green piezoceramic fiber and filling the hole with a conductive fiber. The coaxial fiber is then heated to perform debinding and sintering step.

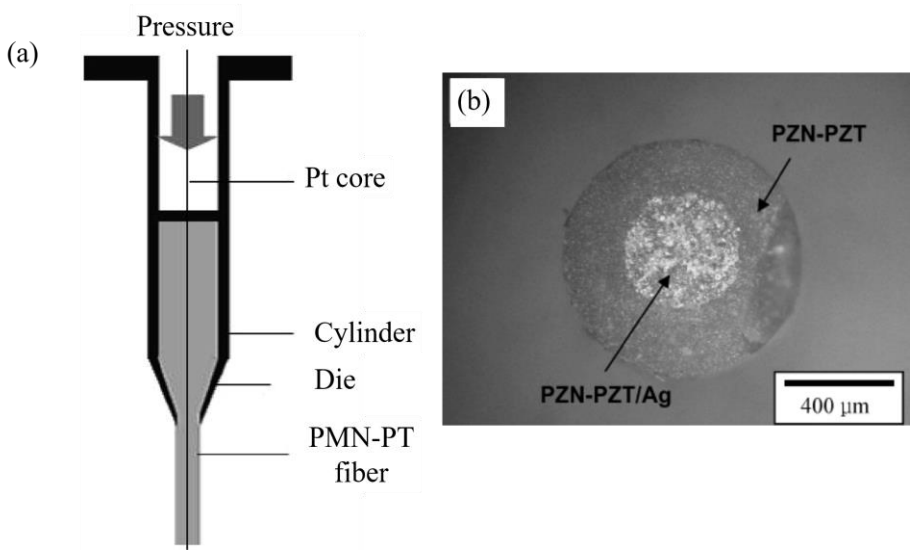

Figure 6. a) Schematic representation of the coextrusion process. The metal core and the piezoelectric paste are extruded simultaneously through two concentric cylinders. b) Image of the cross section of a coaxial fiber after sintering. A hole was drilled into a PZN-PZT green fiber and a conductive cylinder made of PZN-PZT/silver was inserted into the hole. Taken from[99,100] with permission.

Sebald *et al.*[101] and Hajjaji *et al.*[99] studied the morphology and piezoelectric properties of PNN-PZT and PMN-PT, respectively, with a Pt core. They obtained a value of 0.17 and 0.20 for the k_{31} and -112 pC/N and -130 pC/N for the d_{31} respectively. These values are lower than the ones of the bulk ceramic material. They agreed on the same hypothesis to explain this phenomenom: (i) The pressure applied during the process is not high enough to have a dense material. Lower density reduce the material permittivity (ii) The poling process is not effective because of the low aspect ratio of the fiber.

1.2.1.2. Hydrothermal synthesis

The principle of this method is to first seed the conductive core with a precursor solution and then, to perform a hydrothermal reaction to induce the growth of piezoelectric material. This process can be used to make fibers with very small diameter. Indeed, the conductive core

can be of a few microns in diameter and the hydrothermal reaction creates a less than 20 µm ceramic film .[102,103] However, it is difficult to run the process continuously to produce indefinitely long fibers. The process also needs some care because the inner core can suffer from chemical or physical damages during the hydrothermal reaction, which can be performed with harsh chemicals at high temperature. Deterioration of the core can lower the electromechanical coupling of the coaxial fiber. Bowland *et al.*[102,104] studied the influence of the hydrothermal process on the tensile strength and piezoelectric properties of coaxial fibers with a carbon core. To create their coaxial fibers, they functionalized carbon fibers with hydroxyl and ketone groups. Then they seeded the carbon fiber with Titanium based precursors. Finally, a two-steps hydrothermal reaction was performed to synthesize TiO_2, and to convert it into $BaTiO_3$. Figure **7** presents the obtained coaxial fibers. The authors showed that the conversion step has a strong impact on the tensile strength of the fiber. The Young's modulus of coaxial fibers can be as high as 300 GPa, and the tensile strength can exceed 4 GPa. These excellent properties exceed the properties of $BaTiO_3$.[104] They are due to the efficient mechanical reinforcement provided by the carbon fiber core. Keeping the physical integrity of the carbon fiber core is also important for having good piezoelectric properties. The maximum d_{31} they could measure was -12.9 pC/N, which is lower than the -34.5 pC/N[105] of the bulk material. But this measurement was performed for non-yet optimised fiber.[102,104]

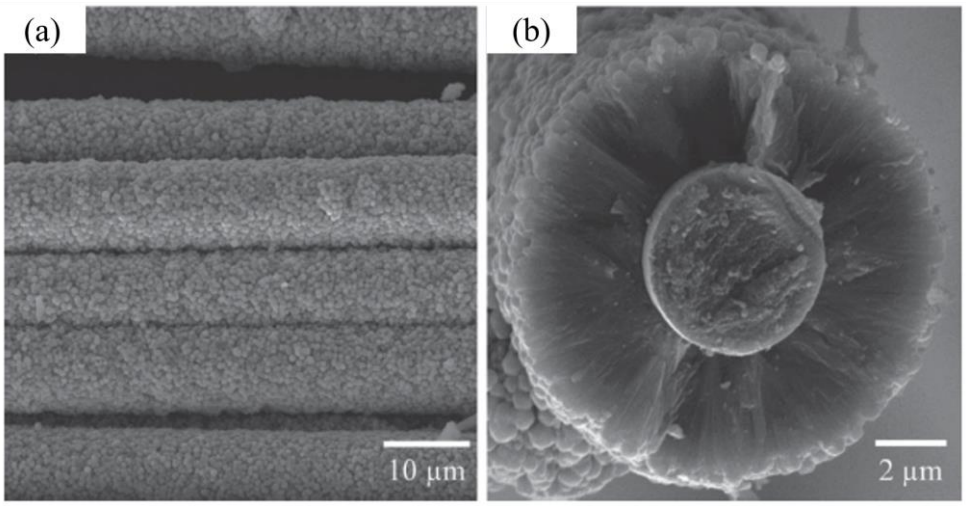

Figure 7. a) Outer surface and b) cross-section of $BaTiO_3$ coated carbon fiber by hydrothermal reaction. Taken from[102] with permission.

1.2.1.3. Electroplating techniques: electrophoresis deposition and electrolytic deposition

Two main techniques exist to create a ceramic layer on a conductive fiber by electroplating: electrophoresis deposition (EPD) and cathodic electrolytic deposition (CELD).[106–112] Materials made by these methods are generally porous and have to be densified. The thickness of the deposited layer does not exceed 200 µm in general.[113]

The EPD technique relies on the motion of charged colloidal particles towards an electrode of opposite charge under a DC field. The core fiber acts as electrode, and the colloidal particles are the piezoelectric particles (Figure 8a). For a homogenous, cracks and voids free, deposition, a dilute and stable colloidal suspension is needed. Kim *et al*.[114] created a PZT coated SiC fiber by the EPD technique. Lin and Sodano[115] synthetised $BaTiO_3$ coated SiC fibers of different aspect ratios. They showed that the effective d_{31} coefficient increases with increasing the aspect ratio (Figure 8b). The maximum obtained d_{31} was about 34 pC/N for an aspect ratio of 0.67. This value is close to the coefficient of bulk $BaTiO_3$ reported in literature.[116]

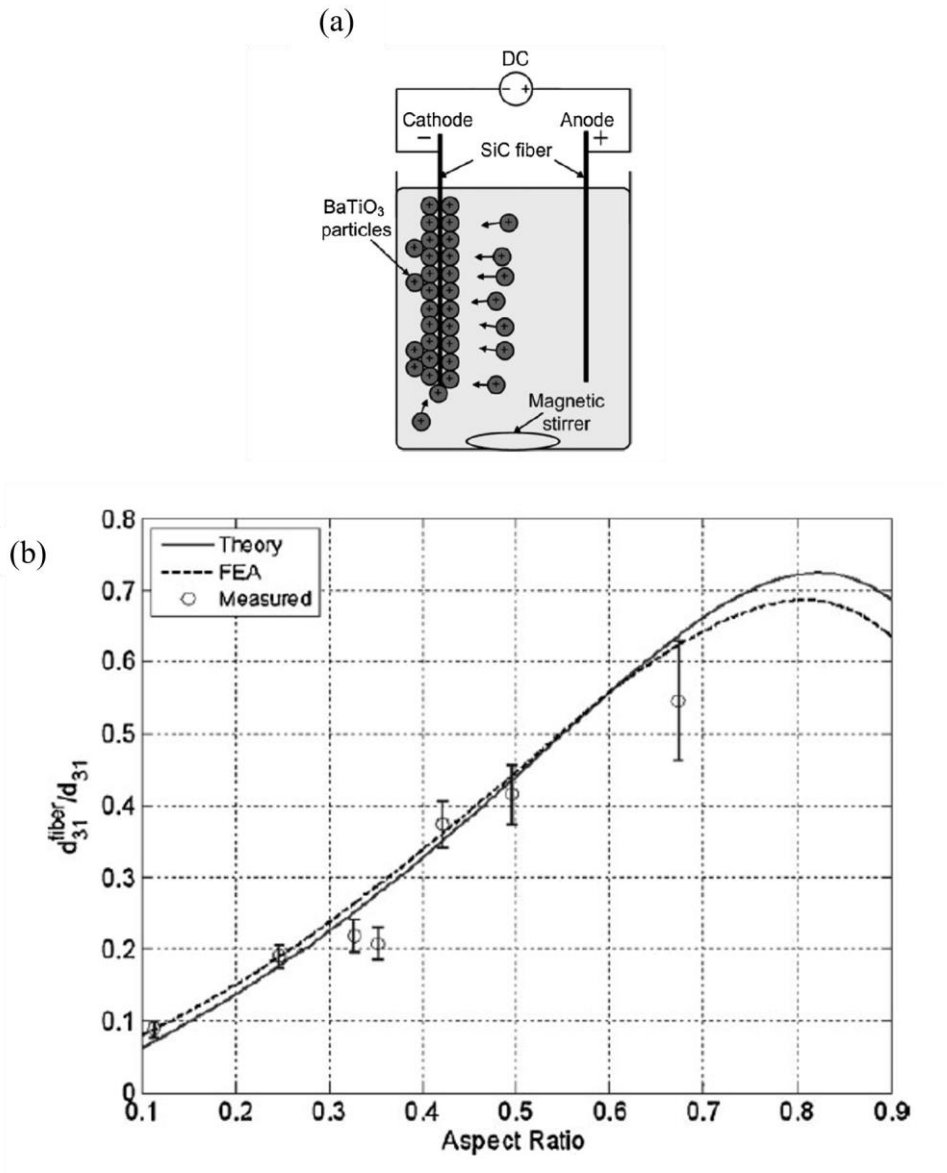

Figure 8 . a) Schematic representation of the EPD process. b) Normalized d_{31} coefficient vs the aspect ratio of the $BaTiO_3$ coaxial fiber made by EPD technique. Taken from[115] with permission.

In the CELD technique, ceramic films are formed from metal salts in solution. [112,116] The pH near the cathode fiber is increased with an electrogenerated base. This induces the hydrolysis and deposition of inorganic materials at the surface of the core fiber. This methods allows a better uniformity and a continuous microstructure compared to the EPD method, but the created films are thinner.[112,117]

1.2.2 Nanowire coated piezoelectric fibers

Fibers coated by inorganic nanowires can still be considered as coaxial piezoelectric fibers even if they operate differently from the fibers described above. Qin *et al.*[118] synthetized ZnO nanowires on a polyaramid fiber core by a hydrothermal method. The bottom layer of ZnO seeds serves as inner electrode. The polar axis of the nanowires is oriented perpendicular to the core fiber as they are grown along this direction. The nanowires are bent with friction between the fiber and another fiber or surface. Current is therefore generated by this friction mechanism. The principle is not expected to be very efficient in terms of piezoelectric activity considering the low piezoelectric coefficient of ZnO[119] and the non-optimized deformation. Nevertheless, nanowire coated piezoelectric fibers can be easily synthesized and implemented in promising applications for energy harvesting[118,120] or damage sensing in composites.[121]

Coaxial fibers can be produced from three different techniques, leading to thicknesses of less than 200 µm for the electroplating techniques and to more than 200 µm for the coextrusion process. There are rather few few studies on coaxial piezoelectric fibers. Such materials have low values of d_{31} compared to the d_{33} of the piezoceramic fibers. In addition, they require a good bonding between the core fiber and the piezoelectric coating to ensure an efficient piezoelectric activity. This point is a critical issue. Nevertheless, coaxial fibers have better mechanical properties than ceramic fibers and remain promising considering their easy poling and implementation in applications and devices.

2. Organic piezoelectric fibers

Piezoelectric polymer fibers are extensively investigated for two main reasons. First, their flexibility make them more processable and better candidates than ceramics for wearable technologies. Second, they can be easily spun from well established melt or wet fiber spinning

techniques. Several polymers including poly(vinyl difluoride) (PVDF), polyamide (PA), polyacrylonitril (PAN), poly(vinyal chloride) (PVC), polylactic acid (PLA) and others display piezoelectric properties.[122,123] PVDF presents a d_{33} up to -30 pC/N.[123] This value remains low compared to piezoceramics but rank among the best in organic materials.

2.1. Piezoelectricity in polymers and in PVDF

The most commonly used piezoelectric polymers are semicrystalline. The presence of a polar crystal phase is necessary to induce piezoelectricity. In PVDF, the crystalline fraction varies typically from 35 to 70%.[124]The orientation of the dipoles can be achieved by thermal annealing, mechanical stretching and high voltage treatments. PVDF[125] and its copolymers, including poly(vinylidene fluoride-co-trifluoroethylene) (PVDF−TrFE), poly(vinylidene fluoride-co-chlorotrifluoroethylene) (PVDF-CTFE) and poly(vinylidene fluoride-hexafluoropropylene) (PVDF-HFP), have at least three polymorphic phases: α, β and γ, presented in Figure 9. The α-phase is the only non-polar phase of PVDF and is the most stable at room temperature. But the β-phase can be obtained upon mechanical stretching of the α and γ phases.[126] PVDF−TrFE, PVDF-CTFE and PVDF-HFP can spontaneously solidify in the β-phase after melting

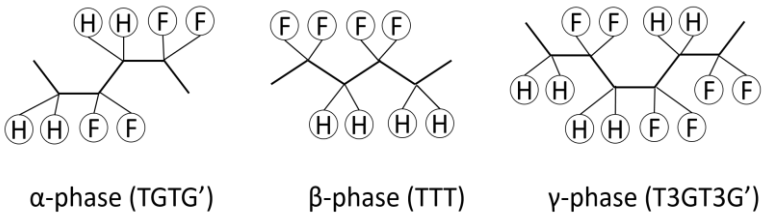

Figure 9. Schematic representation of polymer chain conformation in the different crystal phases of PVDF.

The polarization of the β-phase is achieved by electrical treatment at room or high temperature with a poling field of at least 200 kV/cm.[126] Converting α to β phase is also possible

by means of higher electric field of few MV/cm.[126,127] Contact and corona poling are the mostly used methods to polarize piezoelectric organic films. The polarization conditions are known to strongly affect the piezoelectric coefficients of thin films.[128] The same can be expected for fibers. However, to our knowledge, the piezoelectric coefficients of piezoelectric fibers have not yet been directly measured.

The sign of the piezoelectric coefficients is another distinctive feature of piezoelectric polymers. Indeed, PVDF and its copolymers display a negative d_{33} whereas most inorganic materials have a positive d_{33}. Inorganic materials expand when a field is applied along the polarization direction. This effect can be understood by considering the structure of the ionic lattice of inorganic piezoelectric materials.[1] However, the underlying mechanisms to explain a negative longitudinal piezoelectric coefficient of polymers have been debated over the last years. Contraction of the material upon application of an electric field along the polarization direction has been ascribed to specific responses of either the crystalline parts[129] or volume changes of the amorphous parts of the semi-crystalline polymers.[130,131] According to recent progresses in the field,[132] both parts of the semicrystalline polymer have in fact to be considered to correctly describe the response of piezoelectric polymers for a large range of applied electric fields.

2.2. Polymer fiber spinning process

2.2.1. melt-spinning

In this process, PVDF or multicomponent preformed layers[133,134] are melted above their melting temperature.[135,136] The molten polymer is then extruded trough a die, air quenched to solidify and taken-up on drums (Figure 10a). The crystallinity is controlled by the melt draw ratio[135] which is the speed ratio from the extruder to the first take-up roll. Cold[135] or hot[137] drawing is finally applied to increase the electroactive phase fraction. Fiber spinning of melted PVDF induces a chain orientation and produces mainly non polar α-phase.[135,138] Thermal

drawing, stretching, electrical polarisation or incorporation of fillers can be used to induce the formation of the piezoelectric β-phase of the PVDF. The crystallization and enhancement of the β-phase content of films have been extensively studied in the case of PVDF.[139,140]

Chapron *et al*.[137] monitored the crystallinity of PVDF during the melt spinning process. Figure 10b shows their main results: α to β phase conversion increases with the hot drawing ratio. This conversion can be close to 100%.[141] Yang *et al.*[142] achieved enhancement of the mechanical properties of PVDF fiber by drawing, and obtained a Young modulus of 1.6 GPa and a tensile strength of 119 MPa. Polarisation of the PVDF with a high electric field during stretching improves the β-phase content and can be included in this continuous process.[143]

(a)

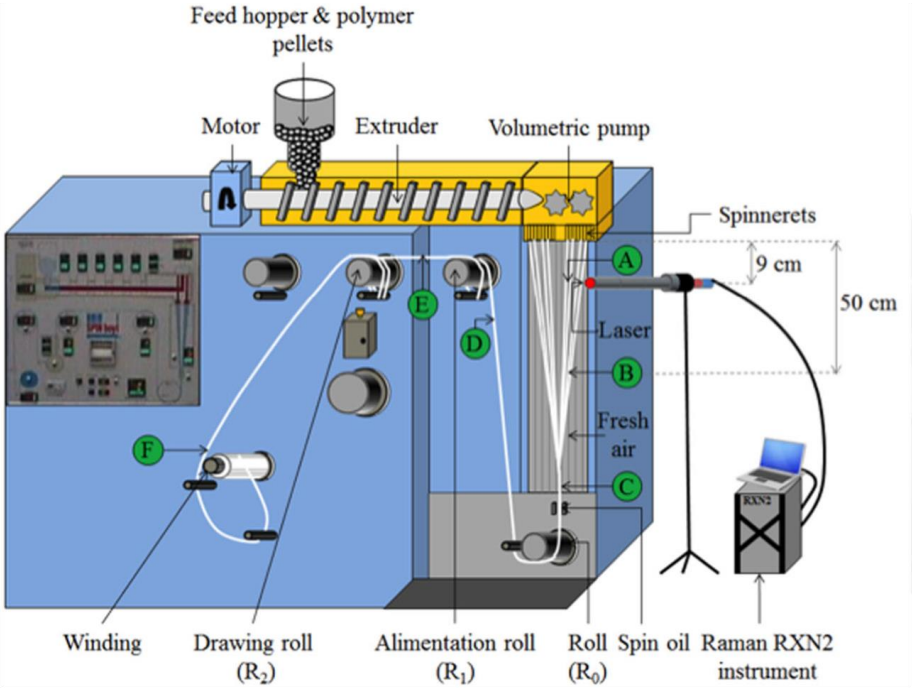

(b)

	λ = 1.25				λ = 4			
			In crystal phase				In crystal phase	
Positions	F_{am}(%)	F_{cryst} (%)	F_{α} (%)	F_{β} (%)	F_{am}(%)	F_{cryst} (%)	F_{α} (%)	F_{β} (%)
A	100	0	—	—	100	0	—	—
B	91	9	100	0	89	11	100	0
C	67	33	100	0	64	36	98	2
D	65	35	100	0	68	32	97	3
E	63	37	100	0	42	58	30	70
F	54	46	100	0	45	55	33	67
Micro-Raman	52	48	99	1	40	60	29	71

Note: Micro-Raman measurements were done on samples after 2 months.

Figure 10. a) melt-spinning system used by Chapron *et al.*[137] b) In-situ Raman measurement showing the evolution of the crystallinity and of the α and β phases content. The positions referred to those shown in a) λ is the draw ratio between *R1* and *R2* at 110°C and 90°C respectively. Taken from[137] with permission.

Adding fillers can also increase the electroactive phase content and improve the stiffness of the fibers.[142] Fillers are used as nucleating agents to promote crystallization.[136,144,145] High aspect ratio fillers can be prefered because of their higher interfacial interaction.[142] Panda *et al.*[136] drawn a PVDF fiber with a crystalline fraction of 74% including 90% of β-phase by adding 0.5%wt of zinc oxide nanorods. The nanorod loading is nevertheless limited because the

extrusion becomes difficult with a high viscosity blend at loading over 10%wt.[124,133,172,173] Moreover, improvements of stiffness are often associated to increased brittleness. Fibers loaded with fillers can break during drawing.[136,144] But the β-phase of composite fibers can be created with lower drawing ratio than that needed for neat PVDF.[145] Not all fillers can increase the conversion to β-phase, but oxides[136,146] and carbon nanotubes (CNT)[144] have been used successfully. The PVDF chains wrap the CNTs during melt spinning. This phenomenon is believed to produce donor-acceptor complexes between the electron rich CNTs and the $–CF_2$ dipoles of the PVDF.[144,147] This mechanism limits the chain mobility during the crystallization and stabilizes the less favourable β-phase.

2.1.2. wet-spinning

In the wet-spinning technique, a polymer solution is injected into a coagulation bath containing a bad solvent of the polymer. This bad solvent has still to be miscible with the solution's solvent. After coagulation, the fiber is guided through washing baths to remove solvents (see Figure 11a). The fiber is finally dried and wound. Depending on the diffusion and coagulation processes, various fiber morphologies can be obtained. As presented in Figure 11b, voids are generated during the coagulation of PVDF. This phenomenon is used to make hollow fiber membranes.[148] Mechanical properties of the final fibers are affected by the presence of voids. Drawing during the spinning process increases the mechanical properties.[149] Jeong *et al.*[150] obtained as spun fibers with a tensile strength of 19 MPa. After post treatment to stretch and remove voids they obtained a tensile strength of almost 300 MPa. The crystalline fraction was 73.7%, and the β fraction was 92.9%.

(a)

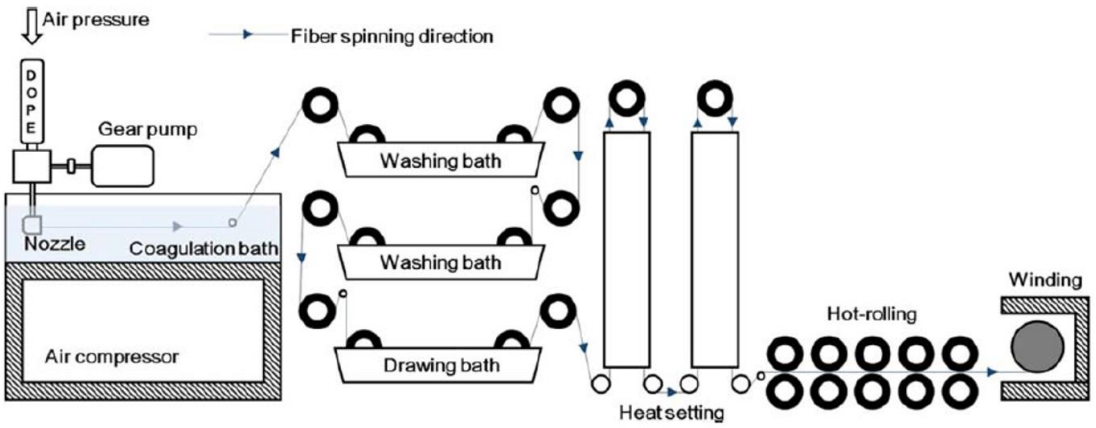

(b)

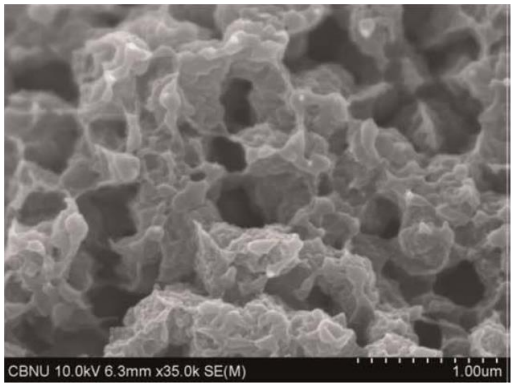

Figure 11. a) Wet spinning system used by Jeong *et al*.[150] The dope, consisting in a solution of 30%wt of PVDF in dimethylacetamide (DMAc), is coagulated into an aqueous solution of 35%wt DMAc at 50°C. The PVDF fiber is then washed in several water baths and drawn in a water bath at 80°C. To remove voids created during the wet spinning process, the PVDF filaments are hot rolled at 130°C. b) SEM images of as-spun PVDF fiber's cross section. With no post treatment, the PVDF fiber is porous. Taken from[150] with permission.

Coagulation in polar solvents and hot drawing promote the formation of β-phase.[150] Increase of the drawing ratio during the coagulation sometimes increases porosity.[151] Drawing in the washing bath over 40°C can also increase porosity. Below this temperature, only the molecular orientation of the amorphous part of the PVDF is affected.[151]

To conclude, the melt-spinning process is a simple and fast method to produce PVDF and PVDF copolymers fibers. But fillers are needed and hot or cold drawing to increase the β phase content. The wet-spinning process produces mainly porous fibers that are mechanically weak, and that often requires post-synthesis treatments to reduce porosity.

2.2. Coaxial fibers

The maximum theoretically predicted calculated value of d_{33} for bulk PVDF is 44 pC/N,[152] which is higher than the one experimentally measured. This difference is attributed to the insufficient poling process. A conductive core is implemented in the fiber to promote the polarization of PVDF, as explained in section Coaxial piezoceramic fibersfor ceramic coaxial fibers.

2.2.1. Coaxial melt spinning and tensile melt extruding

The coaxial melt spinning (or bi-component extrusion) process is based on the extrusion of thermoplastic polymer filled with conductive particles as the core and piezoelectric polymer as the sheath. The advantage of using a thermoplastic core is the possibility to draw it along the PVDF to increase the β-phase content, without breaking the fiber. The fillers have to form a percolated network after drawing so that the core remains conductive,. Studying a PVDF fiber with carbon black filled polypropylene as the core, Lund *et al.*[153] conclude that the resistivity of the core increases with the elongation of the coaxial fiber. Indeed, the conductivity of the core decrease from 0.17 S/cm with no drawing to 0.07 S/cm with a drawing ratio of 3. However, the maximum amount of conductive filler is limited in order to keep the viscosity of the blend sufficiently low to allow fiber spinning. Glauβ *et al.*[154,155] added sodium stearate as a surfactant in a blend of polypropylene and carbon nanotubes to lower the viscosity while being well above the percolation threshold.

The tensile melt extrusion is the extrusion of a melted polymer around a solid conductive core which is guided through a cylinder. The conductivity of the core is not altered by the extrusion process. Using a metal as a core also improves the Young modulus of the coaxial fiber.[156] However, without pre-treatment, the adhesion between the sheath and the metal core is weak,[157] and debonding during mechanical stretching can occur.[156] As for inorganic coaxial fibers, adhesion between the core electrode and the piezoelectric layer is a critical issue.

Fibers made by the above two methods are shown in Figure 12. These methods produce coaxial fibers with good repeatability, are easy to process and scalable. Coaxial fibers made by tensile melt extrusion have a good core conductivity but the adhesion with the sheath is difficult to control. On the other hand, the ones made by bi-component extrusion have a good adhesion but suffer from a low conductivity of the core electrode.

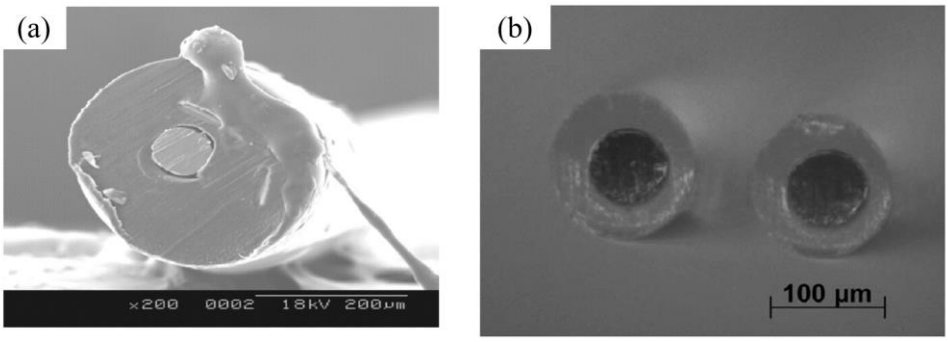

Figure 12. a) Cross section of coaxial PVDF-TrFE/copper coaxial fiber made by tensile melt extrusion. b) Cross section of drawn PVDF/carbon black polypropylene coaxial fibers made by coaxial melt extrusion. Taken from[153,156] with permission.

2.2.2. Electrowetting aided dry spinning

Liu *et al.*[158] proposed a combined process to create PVDF and PVDF-TrFE, coaxial fibers with a copper core. Studies on electrospinning have proven that application of an electric field to a PVDF solution promotes the formation of β-phase nanofibers.[159] In the same way,

electrowetting followed by dry spinning was used to create coaxial fibers. The process is sketched in Figure 13. The solid core, composed of copper and of an insulating layer, is wet by the PVDF charged solution by applying an external electric field (*E1*). The polymeric layer created is elongated through the process and solidifies under an electric field (*E2*). With this technique, the polymer layer thickness falls below 10 µm. Films with a smooth surface, without pores or fractures have been realized with PVDF-TrFE mainly composed of β-phase.

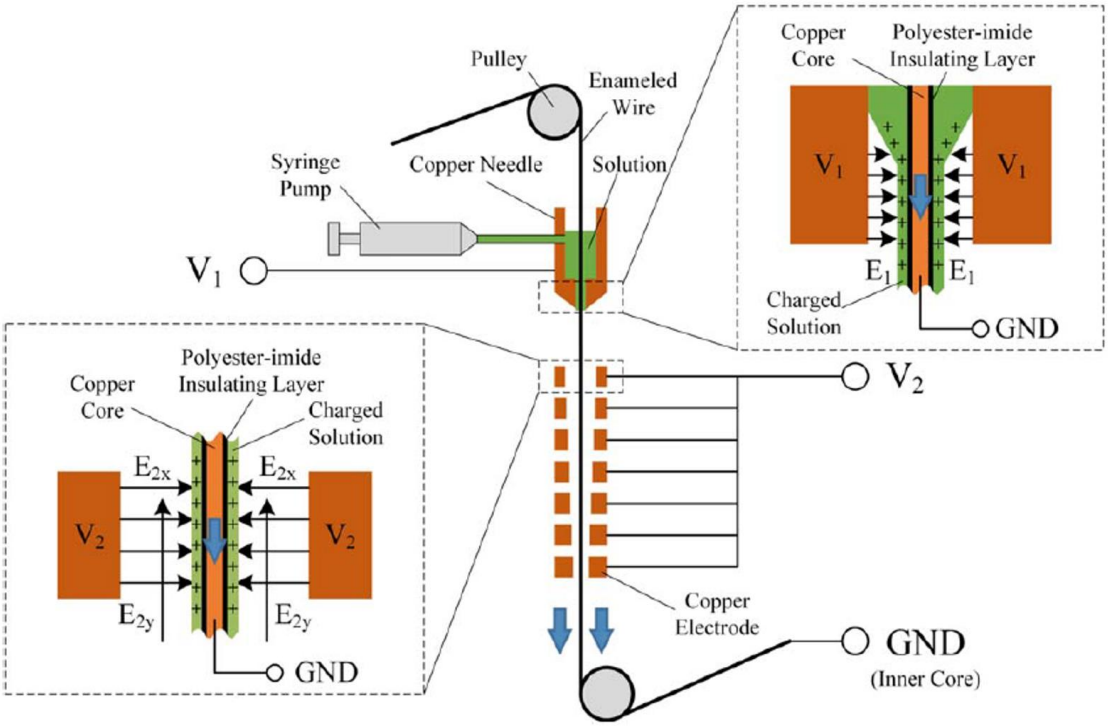

Figure 13. Electrowetting aided dry spinning process proposed by Liu *et al.*[158] The charged solution is composed of PVDF or PVDF-TrFE and a mixture of dimethylformamide (DMF) and acetone. V_1 is 1 kV and V_2 is 4 kV. The insulating layer keeps the charges in the polymeric layer and offers a better adhesion of the PVDF to the conductive core. Taken from[158] with permission.

On one hand, this technique is attractive because it can be used to produce long coaxial fibers with high β phase content with a conductive core that has a good adhesion with the sheath,

without post-treatment. On the other hand, the process is not easily scalable for multifilament production.

3. Piezoelectric composite fibers

Improving the piezoelectric properties of neat piezoelectric materials, be they organic or inorganic, by chemical modification of their composition is becoming increasingly difficult after years of research and optimization. The d_{33} coefficient of PVDF does not exceed -30 pC/N whereas the d_{33} of piezoceramics can exceed 100 pC/N. However, inorganic materials are brittle whereas organic polymers are flexible. The composite approach based on the combination of flexible polymers and highly active inorganic piezoelectric materials appears as a promising way for making new, efficient and mechanically robust piezoelectric fibers. In particular, inorganic piezoelectric particles with high piezoelectric coefficients can be added to passive or electroactive polymers to make flexible piezoelectric fibers. PVDF composites have generally a large amount of piezoelectric fillers and the polymer is only used for its flexibility and permittivity.[160] Recent examples in this field are described in this section.

3.1 Particularity on piezoelectric composite: poling and stress transfer

Piezoelectric performances of composites are usually low compare to neat piezoceramics.[161–163] High loading of particles is needed to significantly increase the d_{33} coefficient. The observed low piezoelectric properties are due to (i) the inefficiency of the poling process due to the low permittivity of the polymer matrix (ii) the poor mechanical stress transfer between the matrix and the piezoelectric inclusions.

High dielectric mismatch between the piezoelectric inorganic filler and the polymeric matrix makes poling of composites difficult to perform. The effective electric field (E_c) seen by the piezoelectric inclusions is lower than the electric field [164] (E_0) applied to the sample and is given by:

$Ec = \frac{3\varepsilon}{2\varepsilon+\varepsilon_c} E_0$, with $\frac{\varepsilon-\varepsilon_m}{\varepsilon+2\varepsilon_m} = \varphi \frac{\varepsilon_c-\varepsilon_m}{\varepsilon_c+2\varepsilon_m}$ in the case of the effective-medium model.[165] ε, ε_c, ε_m are the permittivity of the composite, of the piezoelectric inclusion and of the matrix respectively. φ is the volume fraction of the piezoelectric inclusion. The use of high poling electric fields is limited by the probable composite dielectric breakdown. Increasing the permittivity of the matrix is possible by adding semi-conductive[166,167] or conductive[168–170] fillers. The loading has to be kept below the percolation threshold, else creating short-circuit during poling. Chemical modifications of the particle surface[171–177] can improve the compatibility between the polymer and the particles, creating less defects in the composite and improving its dielectric properties.

Besides difficulties of poling, mechanical stress transfer between the soft matrix and the stiff inorganic inclusions is another critical issue. Using high aspect ratio piezoelectric fillers and aligning them improve the mechanical coupling of the composite and result in higher piezoelectric response.[178–181] Andrew *et al.*[182] improved by more than 200% the d_{33} of 20%vol PZT/PVDF composite films by using nanowires instead of quasi-spherical particles. This effect can be understood by considering the more efficient stress transfer in nanocomposites with high aspect ratio anisotropic nanoparticles.[183] Alignment of anisotropic particles is also important to ensure an efficient stress transfer, and a greater piezoelectric response with the polar axis of the nanoparticles along the axis of piezoelectric activity. Nafari and Sodano[179] demonstrated that a composite made of 40%wt $BaTiO_3$ aligned nanowires with an aspect ratio of 10 in PDMS film has its d_{33} coefficient enhanced by 100% compare with randomly oriented nanowires.

3.2 Composite fiber spinning

Processes to make composite fibers with a polymeric matrix are similar to processes to make polymer fibers (see section 2.2. Polymer fiber spinning process). However, because a

high loading of particles is needed to increase piezoelectric properties, melt-spinning is not the most suitable method. Indeed, the viscosity of the blend increases with the filler content and makes fiber spinning difficult. Usually, the filler fraction does not exceed 10%wt with this technique.[136,145,184,185] Wet-spinning is more appropriate for highly loaded composite fibers.[186–188] Zhang *et al.*[189] succeeded in making polyvinyl chloride (PVC) / $BaTiO_3$ fibers 60 µm in diameter with 50%wt of $BaTiO_3$ nanowires (Figure 14) with a tensile strength of 54 MPa. They also studied the effect of particles anisotropy on the piezoelectric response. The measure of d_{33} was made with a bundle of fibers compressed into the bulk material, cut into cylinder and annealed at 600°C. The poling is made after removing the organic part. They obtained 4.4 pC/N and 13.7 pC/N for spherical particles and nanowires particles respectively.

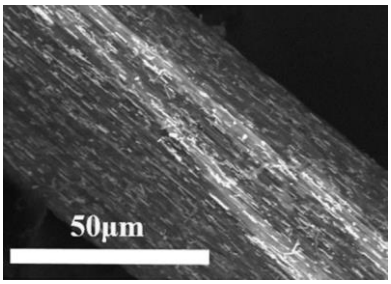

Figure 14. SEM picture of 50%wt $BaTiO_3$ nanowires / PVC fibers.[189] $BaTiO_3$ nanowires were dispersed into a solution of PVC in dimethylacetamide (DMA), wet-spun in a coagulation bath containing a mixture 70:30 DMF / water and drawn in boiled water. Taken from[189] with permission.

More complex hybrid structures, such as conducting wires coated with ZnO nanowires and PVDF, have been proposed.[190] But these structures, even if of cylindrical shape, have large diameters that largely exceed 100 µm. These cylindrical co-axial structures have been shown to display promising properties but are not well suited for smart textile applications because of their large diameter. They are out of the scope of the present review which remains focused on fiber materials meant for composites and smart textile applications.

4. Piezoelectric fibers applications

4.1 From piezoelectric fibers to smart textile structures

Realizing fiber materials with good mechanical and electromechanical properties is the first key challenge towards smart textile applications capable of converting mechanical energy into electrical energy. These textiles could find countless applications as sensors or energy harvesters in clothing, biomedicine, housing, furniture, technical textiles and so on.[45–47] However, this first challenge is not sufficient in itself. Indeed, implementing the fibers in textile structures is also particularly challenging. It is possible to make smart textiles by embedding straps, films or mats of electrospun nanofibers into a textile.[191,192] But, these multilayers structures are not ideal in terms of comfort, flexibility and wearability. Instead, using piezoelectric microfibers that act as both structural and active elements display significant advantages. First microfibers because of their large surface area, compared to 2D films, could in principle generate more charges when mechanically deformed. Second, fiber materials are of interest because of their low flexural rigidity, which scales as the 4^{th} power of their diameter. However, using piezoelectric fibers raises technical difficulties for their poling and electrical connections to conditioning circuits. It is indeed necessary to realize efficient electrical connections that can sustain repeated deformations. These connections are supposed to cover the greatest surface area possible of the active elements to maximize electromechanical transduction. It is also important to avoid shorts-circuits and to properly separate electrode materials.

In spite of these difficulties, exciting advances have been achieved over the last years. Several groups have indeed successfully implemented piezoelectric fibers in textile structures by using methods potentially scalable, and compatible with conventional textile technologies of weaving and even knitting and braiding. We review in this section these recent progresses and discuss their main advantages and limitations.

4.1.1 Woven, braided and knitted single component fibers

We consider in this section polymer piezoelectric fibers made of a single component. These fibers can be produced more easily than co-axial and bi-component fibers. They also display high piezoelectric activity and do not suffer from the delicate adhesion between an inner and outer layer. These single-component fibers are produced by easily scalable methods and can also be implemented in textile structures by already well established technologies. In particular, weaving, knitting and braiding are the three conventional techniques to create a fabric. The possible patterns are almost infinite. Beyond their aesthetic aspect, these patterns differ in their mechanical and physical properties. Figure 15 is an overview of the different dimensions and fabrics that exist from 0D to 3D fabrics. Nonwoven layers are made from electrospun fibers and are out of the scope of this review. 2D and 3D fabrics are woven, braided or knitted fibers or yarns. The active fibers have to be electronically connected in order to exchange charges with a conditioning circuit, be it for polarization or exploitation of piezoelectric activity.

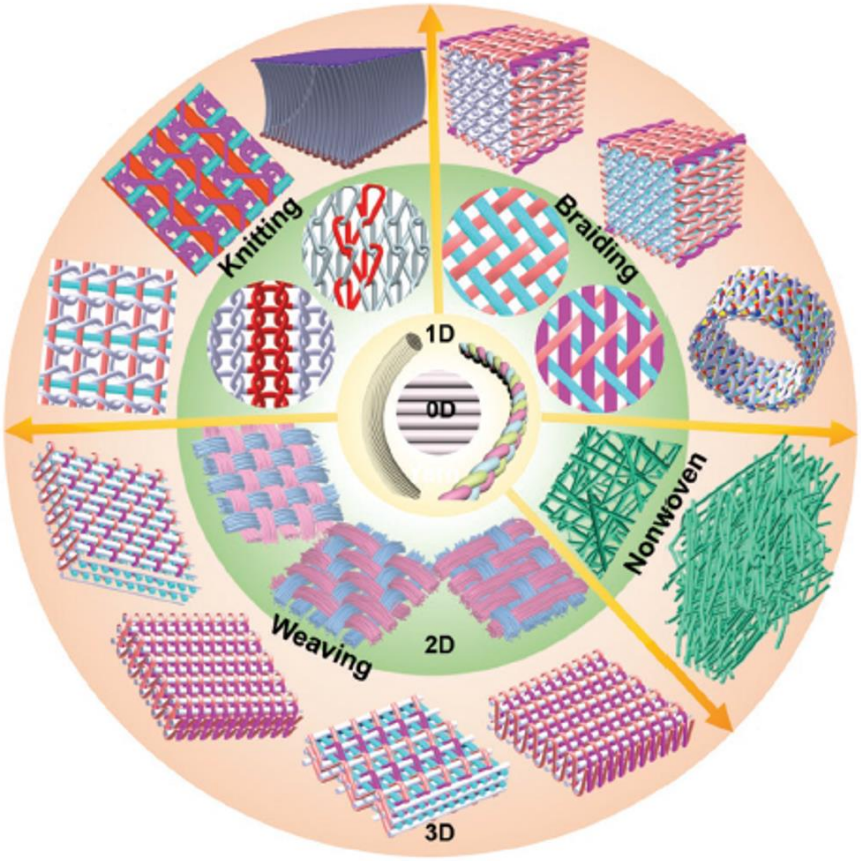

Figure 15. Classification of manufacturing techniques and structural dimensions of textiles. 0D fibers are obtained by the process techniques detailed in the previous sections. 1D yarns are filaments processed by twisting, winding and compounding techniques. 2D and 3D fabrics are woven, knitted or braided 1D yarns. Nonwoven 2D and 3D fabrics are stacked multilayer filaments. Taken from[45] with permission.

Electrodes materials needs to be protected and separated properly to avoid shorts-circuits. Short-circuits can indeed happen if the textile is wet or if the conductive fibers are in contact to each other. Spacers between the electrodes can be used to avoid such short-circuits. Krajewski *et al.*[193] for example worked on PVDF based woven 2D textile. They showed that the number of spacers between conductive electrodes have a strong impact on the output generated voltage. Implementation of spacers make the materials more robust in terms of

protection against shorts. However, it decreases the efficiency of the piezoelectric activity. The use of one spacer instead of two increased by more than 4 times the generated signal.

The output performance of the piezoelectric textile is strongly dependent on the electrodes efficiency. A good contact between the electrodes and the piezoelectric fibers is needed.[193] The resistance of the electrodes has to be as low as possible to limit ohmic losses. The electrodes can be used to *in-situ* polarize the piezoelectric fibers. But poling can also be performed during the fiber spinning thanks to corona method[194,195] or after the manufacturing technique.[196,197] In the latter approach, the piezoelectric fibers are generally working in the d_{31} mode. Electrodes can be used as interdigitated electrodes to work in the d_{33} mode. Zhang *et al.*[197] created a hand-knitted 2D PVC/BTO nanowires composite fiber (Figure 16). Cotton threads are used as a spacers between the Cu wire electrodes. The electrode wires are used to perform poling as interdigitated electrodes. This device was used to harvest energy from the motion of a human arm with an output power of 10.02 nW and a 80 MΩ resistance load. This fiber based material has to be attached onto an adhesive tape to fix the electrodes. It is indeed critical that the electrodes remain perfectly fixed relative to the piezoelecric fibers, so that the electrode location can match the patterns of polarization. This approach seems therefore limited for application in large and deformable textile structures. In addition, the tensile strength of the composite fiber is only of 54 MPa,[189] which can be insufficient for textiles sustaining large stress in applications.

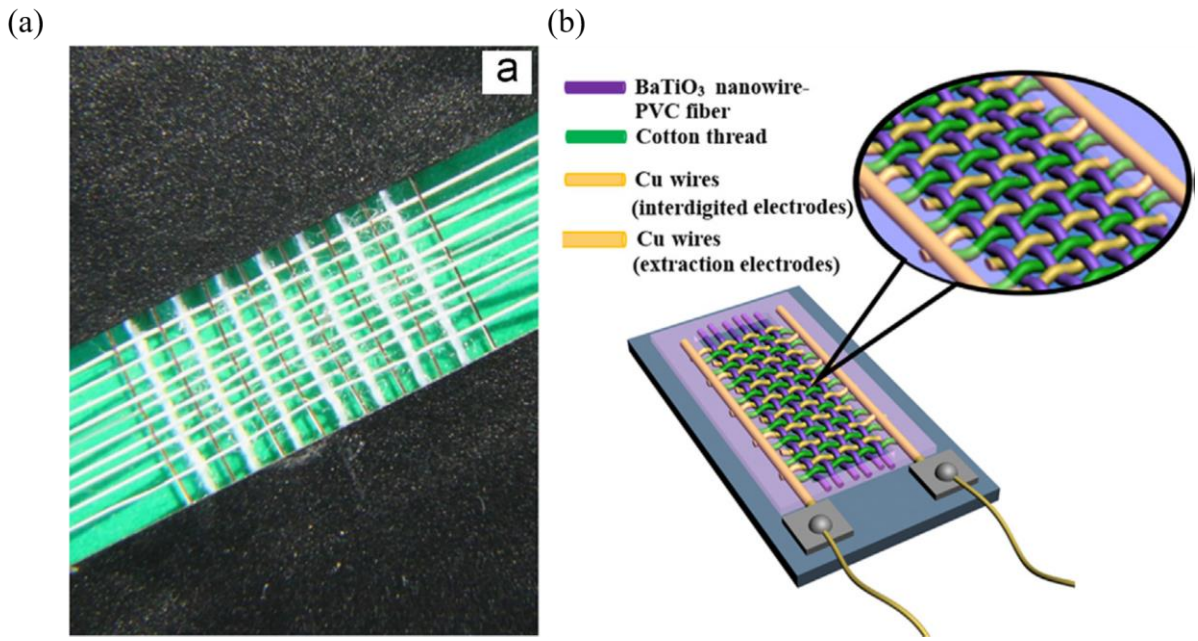

Figure 16. a) Photo and b) schematic representation of the 2D hand-knitted fabric made by Zhang *et al*.[197] The piezoelectric fiber is made of $BaTiO_3$ aligned nanowires in PVC, the cotton thread is used as a spacer to avoid short-circuit..The conductive yarns are used as interdigitated electrodes to perform direct contact poling. The poling was performed at 70°C during 20h with an electric field of 4kV/mm. The output voltage and current of the fabric reached 1.9 V and 24 nA respectively. Taken from[197] with permission.

Increasing the density of the fabric from 2D to 3D can enhance the generated power. Talbourdet *et al*.[196] created woven PVDF melt-spun fiber textiles in 2D and 3D. The 3D fabric presented an output voltage 16 times higher than the 2D fabric. Soin *et al*.[143] created 3D spacer textiles with knitted PVDF fibers sandwiched between conductive yarns. Thanks to this improved designed and better electrical contacts, the fabric could can deliver a power density of 5.07 $\mu W/cm^2$.

The patterns of woven, braided or knitted fabrics are not yet rationally designed to achieve the best output properties. Nevertheless, empirical comparisons provide valuable

insights. In particular, Mokhtari *et al.*[185] created PVDF/$BaTiO_3$ composite fibers and used these fibers in different textile structures. The fibers have a Young modulus of 891 MPa. They can be easily processed by conventional technologies to obtain 2D woven, braided and knitted textiles (Figure 17a,b,c). The authors could compare the force sensitivity and the output power density of the three fabrics. Figure 17c shows this comparison. The knitted textile is found to be the most efficient in terms of sensivity and power generated.

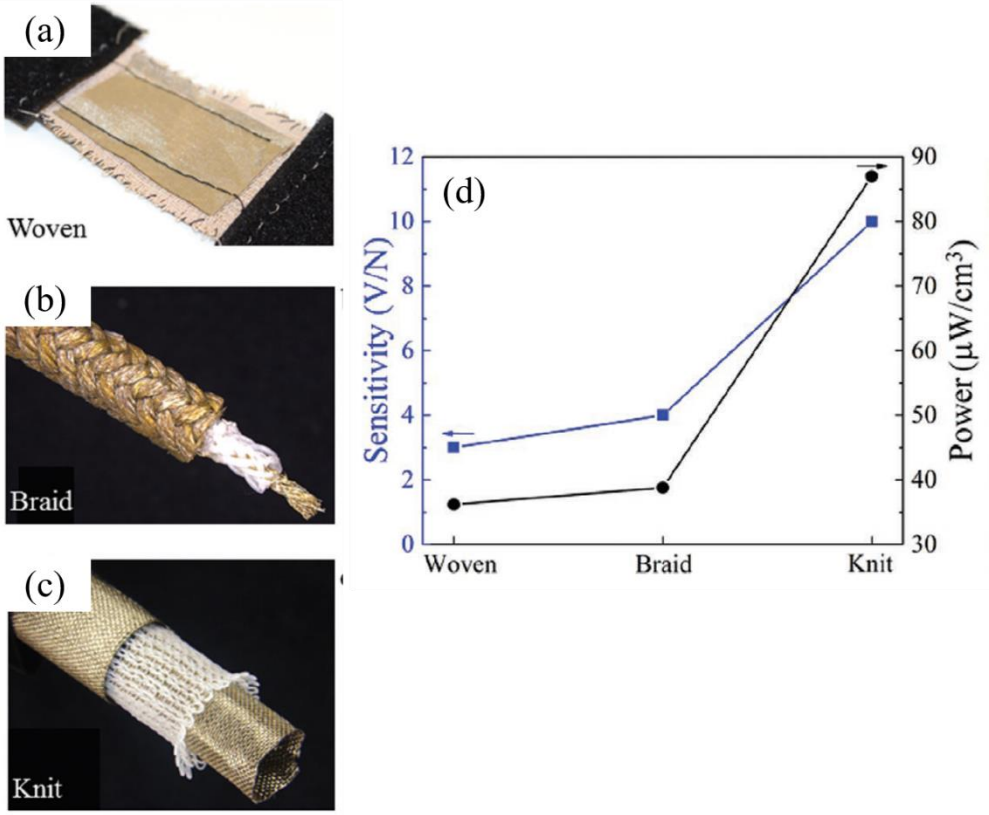

Figure 17. Picture of the a) woven, b) braided, c) knitted 2D textile with composite $BaTiO_3$/PVDF fibers. d) Comparison of the force sensitivity and the power density output of the three fabrics. The fibers were radially poled. Taken from[185] with permission.

Piezoelectric textile structures are often used in laboratory experiments in model deformation modes. They are not always tested and designed in view of specific deformations

met in actual applications. Nevertheless, recent researches have focused on the optimal design of textile structures to display efficient responses to biomechanical deformations.[194] Tajitsu[198,199] spun highly oriented poly(L-lactic acid) (PLLA) fibers. The fibers were used to make plain, twill and satin woven fabrics with conductive carbon fibers and insulating poly(ethylene terephthalate) fibers. A textile prototype was developed for sensing simple human body motions. The PLLA fibers, because of their specific shear piezoelectricity, provide a response in the case of bending for the plain weave, twisting for the twill weave and stretching or highly twisting for the satin weave. The fabric was then used as a sensor on a human arm. The generated signal was transferred to a humanoid robot through an electronic system. The humanoid robot could mimic arm bending and wrist twisting.

4.1.2 Coaxial fiber textiles

Coaxial fibers are of great interest to prevent short-circuiting problems that can occur with single component fibers. There are fewer issues to use them under wet conditions.[200] Co-axial fibers are also more versatile because they can be connected to the electrical circuits by different methods. The outer electrodes can be made of conductive fibers or of printed or coated layers. Åkerfeldt *et al*. studied the durability and washability of PVDF coaxial fibers with coated[201] or printed[202] electrodes. The fibers were coated with poly(3,4-ethylenedioxythiophene):poly(styrene sulfonate) (PEDOT:PSS). They were also printed on a sensing embroidered glove. The coated electrodes were degraded after 1000 shear flexing cycles. Nevertheless, the resistance of the printed electrodes was still below 100 Ω after 100 strain cycles for a strain of 10%. The authors also showed that washing could be performed without affecting too much the resistivity.

Lund *et al*.[200] studied the effect of weaving pattern for three different 2D woven structures made of coaxial PVDF based fibers and conductive yarns used as electrodes (Figure

18). They showed that a good contact between the fibers and the electrodes enhance the voltage generated by the fabric. But they did not succeed to perform an appropriate corona poling with weft rib woven fabrics. The problem was due to the conductive yarns that acted as electromagnetic shield during poling. In a practical case, the twill fabric used as a shoulder strap of a laptop case could generate a power density of 0.08 µW/cm^2. This value is low and still insufficient to power smartphone devices for example which require power level on the order of W. However, they can already be sufficient to power various kinds of sensors, including biomedical sensors, and their communication with computer nodes.

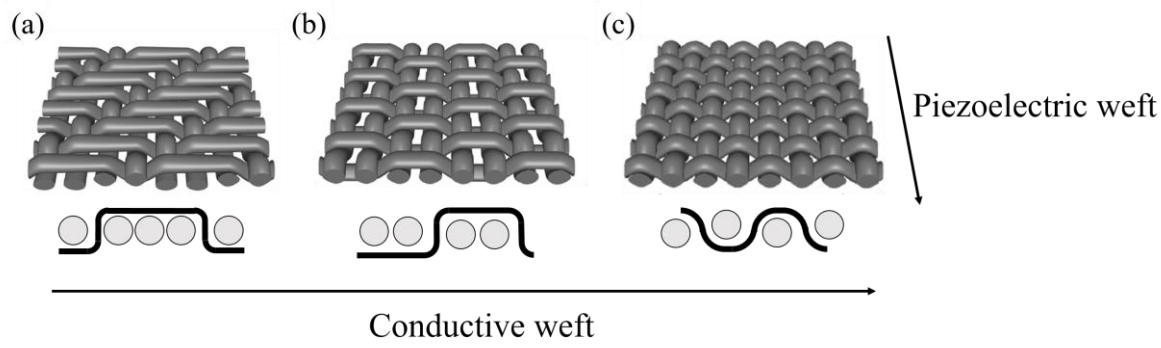

Figure 18. Three different woven patterns made from PVDF and carbon black/polyethylene coaxial fibers (piezoelectric weft) and different conductive yarns. a) Twill b) Weft rib c) plain weave. Adapted from[200] with permission.

4.2 Applications of inorganic piezoelectric fibers

AFC are made of spun piezoelectric fibers embedded in polymer matrices (see section 1.1.2.1). They are reminiscent of so-called MacroFiber Composites (MFC), which are composed of thin rectangular rods, dice-sliced from monolithic PZ materials. AFC and MFC are made by very different processes but still share common applications because of their reminiscent structures. Indeed, AFC and MFC can be used in many applications,[85,203–207] including energy harvesting, structural health monitoring of composites, vibration control and damping, and actuators. MFC have been developed to a commercial stage,[208] and are not

considered in this review because they are not based on actual piezoelectric fibers. AFC are still at an earlier stage of development but enjoy a very promising potential considering their processing from fibers which can be produced by low cost and easily scalable processes of fiber spinning. Their potential applications are described below.

4.2.1 Structural health monitoring (SHM)

The basic concept of SHM is to monitor the structural integrity of a composite structure. Piezoelectric materials can be used for electromechanical measurements[84,209] and acoustic emission[210,211] (AE) to monitor defects of a structure. The AFC is located inside the structure or attached onto the surface. A good adhesion between the host structure and the piezoelectric element is needed in order to have a large sensing area. The AFC is not replaceable in case of defect if it is located inside the structure. The advantage of using AFC instead of monolithic piezoelectric material is that they are more flexible and so can be bonded to curved surfaces.

These methods are non-destructive. In impedance measurements, a stress wave is generated and its response is detected by piezoelectric actuators/sensors. The mechanical impedance of the structure is correlated to the electrical impedance of the piezoelectric device. If the structure is damaged, the electric response is modified compared to a baseline measurement. In AE method, the damage-detection is continuously measured. Vibrations associated to the formation of cracks and defects are detected by the piezoelectric device. Groo *et al.*[121] compared the performance of a coated aramid fabric with ZnO nanowires with traditional AE device, composed of a high frequency microphone that detect damages through airborne acoustic. The piezoelectric fabric is sandwiched between two electrodes made of carbon fiber fabrics and bonded to it with a resin. The sensing ability of the sample is evaluated by a three-point bending test (Figure 19a) and tensile test (Figure 19b). The authors also compared the performance of the piezoelectric device with a sample made without ZnO nanowires. Matrix failure, interfacial

debonding, delamination and fiber failure was detectable by the piezoelectric device. However, a clear distinction of these events remains difficult.

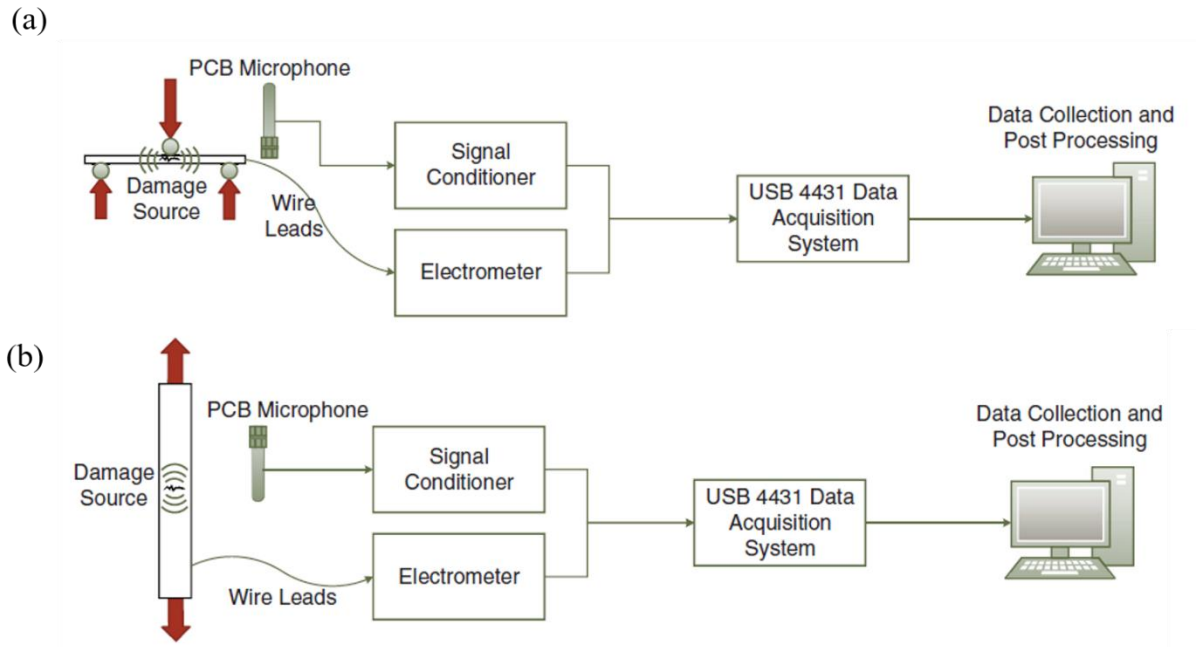

Figure 19. Schematic representations of the a) three-point bending test and b) tensile test on the aramid fabric coated with ZnO nanowires. Taken from[121] with permission.

Piezoelectric fiber based devices for SHM suffer from limitations: the bonding quality to the structure, the maximum strain or flexion of the device before failure and the fatigue and loss of efficiency at high temperature.[212,213]

Bowen *et al.*[214] studied the possible fracture of AFC made of PZT fibers in epoxy matrices. By using a mixing law, they predicted that a minimal composite strength of the AFC exist for a volume fraction of 0.58 of PZT fibers. Below this volume fraction, the fibers break in the matrix. Above this volume fraction, the overall AFC is fractured. Note that the sensor can still be active, even if less efficient, when the fibers are broken in the matrix and still connected to IDE. Of course, the sensor becomes inactive when the all structure and the electrical connections are fractured.[215]

Last, we believe that piezoelectric fibers have still a great and unexplored potential for their use in SHM applications. Indeed, piezoelectric fibers can be made of diameter that compare to that of fibers used for mechanical reinforcement, such as glass or carbon fibers. This is why piezoelectric fibers could be embedded in structural composites without generating mechanical weaknesses. This is a critical limitation in some SHM technologies. For example methods based on Fibre Optical Bragg Gratings[216,217] are interesting but suffer from an intrinsic limitation which is the creation of weaknesses in the composites because of the large size of optical fibers compared to carbon or glass fibers. This limitation can be circumvented when using piezoelectric fibers of small diameter.

4.2.2 Active and passive mechanical damping

A piezoelectric material that is subjected to mechanical excitation can be used for vibration control and damping applications. In the case of passive damping,[218,219] mechanical vibrations is converted into electricity. The associated energy is dissipated by joule effect. Groo *et al.*[218] embedded carbon fibers coated with TiO_2 nanowires, or with BTO nanowires, into an epoxy resin. The damping behavior was analyzed by dynamic mechanical analysis. The damping efficiency of the material was correlated to *tan(δ)*, defined as the ratio of the loss and storage moduli. There was an increase of 62% of the *tan(δ)* at the T_g of the matrix of the BTO based sample compare to the TiO_2 based one. To show more clearly the damping behavior, the different sample beams were mechanically excited with an impulse and their tip velocity was recorded with a laser vibrometer. To compare the samples, the tip velocity is normalized by the maximum velocity for each sample at time 0. The decay of the vibration amplitude with time can be seen in Figure 20. The decay is found to be significantly faster for the BTO based sample. This faster decay confirms the interest of using piezoelectric fibers for vibration damping applications.

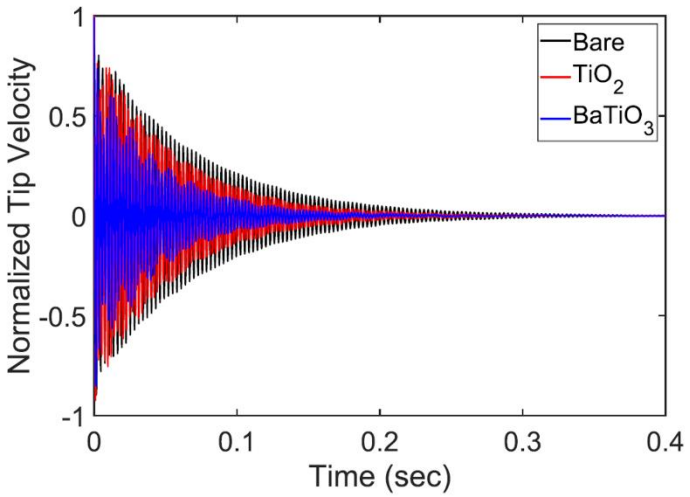

Figure 20. Comparison of the time response of the AFC tip velocity from a mechanical impulse. The bare sample is AFC with only carbon fibers. Taken from[218] with permission.

Piezoelectric materials allows even active damping. This active damping is based on the sensing of vibrations associated to a close-loop actuation system to increase the damping effect.[219] This appealing approach has been the topic of several theoretical studies with AFC.[220–222] However, to our knowledge, the concept has not yet been experimentally realized with AFC and is still a challenge for future research.

4.2.3 Other applications

AFC could also be used as actuators or as energy harvesting devices but MFC are generally preferred because of their higher performance in these applications.[223–226]-MFC perform better because of the rectangular sections of the active piezoelectric components. The latter can be more efficiently connected to electrodes compared to long cylindrical fibers of AFC. However, AFC could be used in greater structures. Indeed MFC are made by cutting monolithic piezoelectric materials. They can be used only in small devices. By contrast, AFC made of indefinitely long piezoelectric fibers could be used in much greater structures. This is an appealing objective for future work which will certainly raise challenges for the connections and poling of the inorganic fibers, such as for macroscopic textile structures made of inorganic fibers and discussed in the previous sections.

Conclusion

It is clear today that piezoelectric fibers could have multiple applications. These applications are limited only by our imagination, and range from biomedical sensors to energy harvesting in textiles or composites. Their processing has reached a high level in terms of robustness and scalability in particular for organic polymer fibers. The synthesis of inorganic piezoelectric fibers is more delicate but can still considered today as well controlled and scalable for some of them. Structural and mechanical characterizations can also be realized with high accuracy using advanced techniques. These advanced characterizations allows a good understanding of the fiber properties. However, in spite of this advanced knowledge, the characterization of electromechanical properties remains difficult. In particular, measurements of accurate piezoelectric coefficients is still challenging, and relies often on the design of home made instrumentation.

The road to applications of piezoelectric fibers faces many challenges. The first is the realization of fibers with high piezoelectric response. Inorganic fibers meet this criterion but remain difficult to synthesize and to use because of their brittleness. Polymeric fibers are flexible and robust. They can be produced by processes inspired by industry. However, their piezoelectric response remains weak. The ideal solution could come from nanocomposite fibers composed of inorganic inclusions in polymer fibers capable of coupling deformability and strong piezoelectric response. This is clearly a promising area for future research. The fundamental questions to be solved will concern the polarization of such systems and the achievement of efficient stress transfer between piezoelectric nanoparticles and polymeric matrices. The integration of fibers into functional textiles and composites is the second major challenge associated with the development of piezoelectric fibers. The realization of co-axial fibers offers many advantages for optimal polarization and integration into electroactive fabrics. However, bi-component fibers remain difficult to produce. The adhesion between the

conductive core and the piezoelectric outer layer is also an important issue. Finally, the integration of piezoelectric textiles in real applications will require the design of optimized structures to generate the best electromechanical transduction in response to a given deformation. Modeling work will certainly be of great interest at this level to predict the preferred weaving structures. The processing of piezoelectric fibers remains a fascinating field with major technological objectives but also scientific challenges from chemistry to electrical engineering through materials science and biomechanics.

Corresponding Author

Philippe Poulin

philippe.poulin@crpp.cnrs.fr

Author Contributions

The manuscript was written through contributions of all authors. All authors have given approval to the final version of the manuscript.

Funding Sources

This study received financial support from the French government in the framework of the University of Bordeaux's IdEx "Investments for the Future" program/GPR PPM.

ANR Funding POETICS project ANR-17-CE05-0004-01

(1) Jones, D. J.; Prasad, S. E.; Wallace, J. B. Piezoelectric Materials and Their Applications. *Advanced Ceramic Materials: Applications of Advanced Materials in a High-Tech Society I*, 1996, *122–1*, 71–143. https://doi.org/10.4028/www.scientific.net/KEM.122-124.71.

(2) Ghosh, B.; Jain, R. K.; Majumder, S.; Roy, S. S.; Mukhopadhyay, S. Experimental Characterizations of Bimorph Piezoelectric Actuator for Robotic Assembly. *Journal of Intelligent Material Systems and Structures*, 2017, *28*, 2095–2109. https://doi.org/10.1177/1045389x16685441.

(3) Khanbareh, H.; de Boom, K.; Schelen, B.; Scharff, R. B. N.; Wang, C. C. L.; van der Zwaag, S.; Groen, P. Large Area and Flexible Micro-Porous Piezoelectric Materials for Soft Robotic Skin. *Sensors and Actuators a-Physical*, 2017, *263*, 554–562. https://doi.org/10.1016/j.sna.2017.07.001.

(4) Oldham, K.; Pulskamp, J.; Polcawich, R.; Ranade, P.; Dubey, M. Thin-Film Piezoelectric Actuators for Bio-Inspired Micro-Robotic Applications. *Integrated Ferroelectrics*, 2007, *95*, 54–65. https://doi.org/10.1080/10584580701756482.

(5) Zhu, M. M.; Lou, M. N.; Abdalla, I.; Yu, J. Y.; Li, Z. L.; Ding, B. Highly Shape Adaptive Fiber Based Electronic Skin for Sensitive Joint Motion Monitoring and Tactile Sensing. *Nano Energy*, 2020, *69*. https://doi.org/10.1016/j.nanoen.2019.104429.

(6) Wang, X. M.; Sun, F. Z.; Yin, G. C.; Wang, Y. T.; Liu, B.; Dong, M. D. Tactile-Sensing Based on Flexible PVDF Nanofibers via Electrospinning: A Review. *Sensors*, 2018, *18*, 16. https://doi.org/10.3390/s18020330.

(7) Chen, G. R.; Li, Y. Z.; Bick, M.; Chen, J. Smart Textiles for Electricity Generation. *Chemical Reviews*, 2020, *120*, 3668–3720. https://doi.org/10.1021/acs.chemrev.9b00821.

(8) Elahi, H.; Munir, K.; Eugeni, M.; Atek, S.; Gaudenzi, P. Energy Harvesting towards Self-Powered IoT Devices. *Energies*, 2020, *13*, 31. https://doi.org/10.3390/en13215528.

(9) Kanno, I. Piezoelectric MEMS: Ferroelectric Thin Films for MEMS Applications. *Japanese Journal of Applied Physics*, 2018, *57*, 9. https://doi.org/10.7567/jjap.57.040101.

(10) Cook-Chennault, K. A.; Thambi, N.; Sastry, A. M. Powering MEMS Portable Devices - a Review of Non-Regenerative and Regenerative Power Supply Systems with Special Emphasis on Piezoelectric Energy Harvesting Systems. *Smart Materials and Structures*, 2008, *17*, 33. https://doi.org/10.1088/0964-1726/17/4/043001.

(11) Saadon, S.; Sidek, O. A Review of Vibration-Based MEMS Piezoelectric Energy Harvesters. *Energy Conversion and Management*, 2011, *52*, 500–504. https://doi.org/10.1016/j.enconman.2010.07.024.

(12) Khazaee, M.; Rezaniakolaie, A.; Rosendahl, L. A Broadband Macro-Fiber-Composite Piezoelectric Energy Harvester for Higher Energy Conversion from Practical Wideband Vibrations. *Nano Energy*, 2020, *76*. https://doi.org/10.1016/j.nanoen.2020.104978.

(13) Anton, S. R.; Sodano, H. A. A Review of Power Harvesting Using Piezoelectric Materials (2003-2006). *Smart Materials and Structures*, 2007, *16*, R1–R21. https://doi.org/10.1088/0964-1726/16/3/r01.

(14) Beeby, S. P.; Tudor, M. J.; White, N. M. Energy Harvesting Vibration Sources for Microsystems Applications. *Measurement Science and Technology*, 2006, *17*, R175–R195. https://doi.org/10.1088/0957-0233/17/12/r01.

(15) Narita, F.; Fox, M. A Review on Piezoelectric, Magnetostrictive, and Magnetoelectric Materials and Device Technologies for Energy Harvesting Applications. *Advanced Engineering Materials*, 2018, *20*, 22. https://doi.org/10.1002/adem.201700743.
(16) Zeng, W.; Shu, L.; Li, Q.; Chen, S.; Wang, F.; Tao, X. M. Fiber-Based Wearable Electronics: A Review of Materials, Fabrication, Devices, and Applications. *Advanced Materials*, 2014, *26*, 5310–5336. https://doi.org/10.1002/adma.201400633.
(17) Shaikh, F. K.; Zeadally, S. Energy Harvesting in Wireless Sensor Networks: A Comprehensive Review. *Renewable & Sustainable Energy Reviews*, 2016, *55*, 1041–1054. https://doi.org/10.1016/j.rser.2015.11.010.
(18) Bowen, C. R.; Kim, H. A.; Weaver, P. M.; Dunn, S. Piezoelectric and Ferroelectric Materials and Structures for Energy Harvesting Applications. *Energy & Environmental Science*, 2014, *7*, 25–44. https://doi.org/10.1039/c3ee42454e.
(19) Bagherzadeh, R.; Sorayani Bafqi, M. S.; Saveh-Shemshaki, N.; Khomarloo, N. 4 - Advanced Fibrous Materials for Wearable Energy Harvesting Applications. In *Engineered Polymeric Fibrous Materials*; Latifi, M., Ed.; The Textile Institute Book Series; Woodhead Publishing, 2021; pp 93–109. https://doi.org/10.1016/B978-0-12-824381-7.00003-2.
(20) Sezer, N.; Koç, M. A Comprehensive Review on the State-of-the-Art of Piezoelectric Energy Harvesting. *Nano Energy* **2021**, *80*, 105567. https://doi.org/10.1016/j.nanoen.2020.105567.
(21) Lee, C. L.; Park, H.; Lee, J. H. Recent Structure Development of Poly(Vinylidene Fluoride)-Based Piezoelectric Nanogenerator for Self-Powered Sensor. *Actuators*, 2020, *9*, 15. https://doi.org/10.3390/act9030057.
(22) Lin, X. J.; Chen, G. L.; Li, J. N.; Lu, F.; Huang, S. F.; Cheng, X. Investigation of Acoustic Emission Source Localization Performance on the Plate Structure Using Piezoelectric Fiber Composites. *Sensors and Actuators a-Physical*, 2018, *282*, 9–16. https://doi.org/10.1016/j.sna.2018.09.027.
(23) Zhou, W. Y.; Wang, X. M.; Qian, W.; Wu, W. Optimization of Locations and Fiber Orientations of Piezocomposite Actuators on Flexible Wings for Aeroelastic Control. *Journal of Aerospace Engineering*, 2019, *32*. https://doi.org/10.1061/(asce)as.1943-5525.0001049.
(24) Tekpinar, M.; Khayatzadeh, R.; Ferhanoglu, O. Multiple-Pattern Generating Piezoelectric Fiber Scanner toward Endoscopic Applications. *Optical Engineering*, 2019, *58*. https://doi.org/10.1117/1.oe.58.2.023101.
(25) Izyumskaya, N.; Alivov, Y.; Cho, S. J.; Morkoc, H.; Lee, H.; Kang, Y. S. Processing, Structure, Properties, and Applications of PZT Thin Films. *Critical Reviews in Solid State and Materials Sciences*, 2007, *32*, 111–202. https://doi.org/10.1080/10408430701707347.
(26) Kang, M. G.; Jung, W. S.; Kang, C. Y.; Yoon, S. J. Recent Progress on PZT Based Piezoelectric Energy Harvesting Technologies. *Actuators*, 2016, *5*, 17. https://doi.org/10.3390/act5010005.
(27) Acosta, M.; Novak, N.; Rojas, V.; Patel, S.; Vaish, R.; Koruza, J.; Rossetti, G. A.; Rodel, J. BaTiO3-Based Piezoelectrics: Fundamentals, Current Status, and Perspectives. *Applied Physics Reviews*, 2017, *4*, 53. https://doi.org/10.1063/1.4990046.
(28) Martins, P.; Lopes, A. C.; Lanceros-Mendez, S. Electroactive Phases of Poly(Vinylidene Fluoride): Determination, Processing and Applications. *Progress in Polymer Science*, 2014, *39*, 683–706. https://doi.org/10.1016/j.progpolymsci.2013.07.006.

(29) Li, Y. C.; Liao, C. Z.; Tjong, S. C. Electrospun Polyvinylidene Fluoride-Based Fibrous Scaffolds with Piezoelectric Characteristics for Bone and Neural Tissue Engineering. *Nanomaterials*, 2019, *9*, 42. https://doi.org/10.3390/nano9070952.
(30) Lang, S. B.; Muensit, S. Review of Some Lesser-Known Applications of Piezoelectric and Pyroelectric Polymers. *Applied Physics a-Materials Science & Processing*, 2006, *85*, 125–134. https://doi.org/10.1007/s00339-006-3688-8.
(31) Stadlober, B.; Zirkl, M.; Irimia-Vladu, M. Route towards Sustainable Smart Sensors: Ferroelectric Polyvinylidene Fluoride-Based Materials and Their Integration in Flexible Electronics. *Chemical Society Reviews*, 2019, *48*, 1787–1825. https://doi.org/10.1039/c8cs00928g.
(32) Huet, F.; Formosa, F.; Badel, A.; Capsal, J. F.; Lallart, M. Vibration Energy Harvesting Device Using P(VDF-TrFE) Hybrid Fluid Diaphragm. *Sensors and Actuators a-Physical*, 2016, *247*, 12–23. https://doi.org/10.1016/j.sna.2016.05.029.
(33) Chu, B. J.; Zhou, X.; Neese, B.; Zhang, Q. M.; Bauer, F. Relaxor Ferroelectric Polymer-Poly(Vinylidene Fluoride-Trifluoroethylene- Chlorofluoroethylene) Terpolymer High Electric Energy Density and Field Dependent Dielectric Response. *Ferroelectrics*, 2006, *331*, 35–42. https://doi.org/10.1080/00150190600732926.
(34) Mokhtari, F.; Cheng, Z. X.; Raad, R.; Xi, J. T.; Foroughi, J. Piezofibers to Smart Textiles: A Review on Recent Advances and Future Outlook for Wearable Technology. *Journal of Materials Chemistry A*, 2020, *8*, 9496–9522. https://doi.org/10.1039/d0ta00227e.
(35) Jones, F. R.; Huff, N. T. 19 - The Structure and Properties of Glass Fibers. In *Handbook of Properties of Textile and Technical Fibres (Second Edition)*; Bunsell, A. R., Ed.; The Textile Institute Book Series; Woodhead Publishing, 2018; pp 757–803. https://doi.org/10.1016/B978-0-08-101272-7.00019-5.
(36) Newcomb, B. A.; Chae, H. G. 21 - The Properties of Carbon Fibers. In *Handbook of Properties of Textile and Technical Fibres (Second Edition)*; Bunsell, A. R., Ed.; The Textile Institute Book Series; Woodhead Publishing, 2018; pp 841–871. https://doi.org/10.1016/B978-0-08-101272-7.00021-3.
(37) Sawai, D.; Fujii, Y.; Kanamoto, T. Development of Oriented Morphology and Tensile Properties upon Superdawing of Solution-Spun Fibers of Ultra-High Molecular Weight Poly(Acrylonitrile). *Polymer*, 2006, *47*, 4445–4453. https://doi.org/10.1016/j.polymer.2006.03.067.
(38) Vlasblom, M. 18 - The Manufacture, Properties, and Applications of High-Strength, High-Modulus Polyethylene Fibers. In *Handbook of Properties of Textile and Technical Fibres (Second Edition)*; Bunsell, A. R., Ed.; The Textile Institute Book Series; Woodhead Publishing, 2018; pp 699–755. https://doi.org/10.1016/B978-0-08-101272-7.00018-3.
(39) Wang, M. L.; Bian, W. F.; Jiang, Z. C. Estimate of Carbon Fiber's Fracture Toughness Based on the Small Angle X-Ray Diffraction. *Polymer Bulletin*, 2017, *74*, 4143–4151. https://doi.org/10.1007/s00289-017-1941-2.
(40) Binkle, O.; Nass, R. Synthesis and Characterization of PZT Fibers via Sol-Gel. *Journal of Sol-Gel Science and Technology*, 1998, *13*, 1023–1026. https://doi.org/10.1023/a:1008616516686.
(41) Yoshikawa, S.; Selvaraj, U.; Moses, P.; Witham, J.; Meyer, R.; Shrout, T. PB(ZR,TI)O-3 PZT FIBERS - FABRICATION AND MEASUREMENT METHODS. *Journal of Intelligent Material Systems and Structures*, 1995, *6*, 152–158. https://doi.org/10.1177/1045389x9500600202.

(42) Du, C. H.; Zhu, B. K.; Xu, Y. N. A Study on the Relationship between the Crystal Structure and Hard Elasticity of PVDF Fibers. *Macromolecular Materials and Engineering*, 2005, *290*, 786–791. https://doi.org/10.1002/mame.200400327.
(43) Hua, Z.; Ping, R.; Zhang, G. F.; Xiao, C. F. Effects of Stretching Ratio and Temperature on Phase Transition of Melt-Spun Poly(Vinylidene Fluoride) Fibers. *Journal of Wuhan University of Technology-Materials Science Edition*, 2006, *21*, 53–55. https://doi.org/10.1007/bf02841204.
(44) Soin, N.; Shah, T. H.; Anand, S. C.; Geng, J. F.; Pornwannachai, W.; Mandal, P.; Reid, D.; Sharma, S.; Hadimani, R. L.; Bayramol, D. V.; Siores, E. Novel "3-D Spacer" All Fibre Piezoelectric Textiles for Energy Harvesting Applications. *Energy & Environmental Science*, 2014, *7*, 1670–1679. https://doi.org/10.1039/c3ee43987a.
(45) Dong, K.; Peng, X.; Wang, Z. L. Fiber/Fabric-Based Piezoelectric and Triboelectric Nanogenerators for Flexible/Stretchable and Wearable Electronics and Artificial Intelligence. *Advanced Materials* **2020**, *32* (5), 1902549. https://doi.org/10.1002/adma.201902549.
(46) Chen, G.; Li, Y.; Bick, M.; Chen, J. Smart Textiles for Electricity Generation. *Chem. Rev.* **2020**, *120* (8), 3668–3720. https://doi.org/10.1021/acs.chemrev.9b00821.
(47) Mokhtari, F.; Cheng, Z.; Raad, R.; Xi, J.; Foroughi, J. Piezofibers to Smart Textiles: A Review on Recent Advances and Future Outlook for Wearable Technology. *J. Mater. Chem. A* **2020**, *8* (19), 9496–9522. https://doi.org/10.1039/D0TA00227E.
(48) Kalimuldina, G.; Turdakyn, N.; Abay, I.; Medeubayev, A.; Nurpeissova, A.; Adair, D.; Bakenov, Z. A Review of Piezoelectric PVDF Film by Electrospinning and Its Applications. *Sensors*, 2020, *20*. https://doi.org/10.3390/s20185214.
(49) Ebru, M. A.; Dagdeviren, C.; Papila, M. Pb(Zr,Ti)O3 Nanofibers Produced by Electrospinning Process. *MRS Online Proceedings Library* **2009**, *1129* (1), 708. https://doi.org/10.1557/PROC-1129-V07-08.
(50) Azmi, S.; Hosseini Varkiani, S.-M.; Latifi, M.; Bagherzadeh, R. Tuning Energy Harvesting Devices with Different Layout Angles to Robust the Mechanical-to-Electrical Energy Conversion Performance. *Journal of Industrial Textiles* **2020**, 1528083720928822. https://doi.org/10.1177/1528083720928822.
(51) Zaarour, B.; Zhu, L.; Huang, C.; Jin, X.; Alghafari, H.; Fang, J.; Lin, T. A Review on Piezoelectric Fibers and Nanowires for Energy Harvesting. *Journal of Industrial Textiles* **2021**, *51* (2), 297–340. https://doi.org/10.1177/1528083719870197.
(52) Briscoe, J.; Dunn, S. Piezoelectric Nanogenerators – a Review of Nanostructured Piezoelectric Energy Harvesters. *Nano Energy* **2015**, *14*, 15–29. https://doi.org/10.1016/j.nanoen.2014.11.059.
(53) Chandrasekaran, S.; Bowen, C.; Roscow, J.; Zhang, Y.; Dang, D. K.; Kim, E. J.; Misra, R. D. K.; Deng, L.; Chung, J. S.; Hur, S. H. Micro-Scale to Nano-Scale Generators for Energy Harvesting: Self Powered Piezoelectric, Triboelectric and Hybrid Devices. *Physics Reports* **2019**, *792*, 1–33. https://doi.org/10.1016/j.physrep.2018.11.001.
(54) Espinosa, H. D.; Bernal, R. A.; Minary-Jolandan, M. A Review of Mechanical and Electromechanical Properties of Piezoelectric Nanowires. *Advanced Materials* **2012**, *24* (34), 4656–4675. https://doi.org/10.1002/adma.201104810.
(55) Xu, Q.; Wen, J.; Qin, Y. Development and Outlook of High Output Piezoelectric Nanogenerators. *Nano Energy* **2021**, *86*, 106080. https://doi.org/10.1016/j.nanoen.2021.106080.
(56) Zhang, D.; Wang, D.; Xu, Z.; Zhang, X.; Yang, Y.; Guo, J.; Zhang, B.; Zhao, W. Diversiform Sensors and Sensing Systems Driven by Triboelectric and Piezoelectric

Nanogenerators. *Coordination Chemistry Reviews* **2021**, *427*, 213597. https://doi.org/10.1016/j.ccr.2020.213597.
(57) Kechiche, M. B.; Bauer, F.; Harzallah, O.; Drean, J. Y. Development of Piezoelectric Coaxial Filament Sensors P(VDF-TrFE)/Copper for Textile Structure Instrumentation. *Sensors and Actuators a-Physical*, 2013, *204*, 122–130. https://doi.org/10.1016/j.sna.2013.10.007.
(58) Martins, R. S.; Goncalves, R.; Azevedo, T.; Rocha, J. G.; Nobrega, J. M.; Carvalho, H.; Lanceros-Mendez, S. Piezoelectric Coaxial Filaments Produced by Coextrusion of Poly(Vinylidene Fluoride) and Electrically Conductive Inner and Outer Layers. *Journal of Applied Polymer Science*, 2014, *131*. https://doi.org/10.1002/app.40710.
(59) Piezo Material Properties https://piezo.com/pages/piezo-material (accessed 2021 -04 -07).
(60) Piezoelectric Pyroelectric Film | PolyK Technologies http://www.polyk-lab.com/taxonomy/term/7 (accessed 2021 -07 -15).
(61) Heiber, J.; Clemens, F.; Graule, T.; Hülsenberg, D. Thermoplastic Extrusion to Highly-Loaded Thin Green Fibres Containing Pb(Zr,Ti)O3. *Advanced Engineering Materials* **2005**, *7* (5), 404–408. https://doi.org/10.1002/adem.200500052.
(62) Lusiola, T.; Hussain, A.; Kim, M. H.; Graule, T.; Clemens, F. Ferroelectric KNNT Fibers by Thermoplastic Extrusion Process: Microstructure and Electromechanical Characterization. *Actuators* **2015**, *4* (2), 99–113. https://doi.org/10.3390/act4020099.
(63) Sebastian, T.; Lusiola, T.; Clemens, F. Ferroelectric Hybrid Fibers to Develop Flexible Sensors for Shape Sensing of Smart Textiles and Soft Condensed Matter Bodies. *Smart Mater. Struct.* **2017**, *26* (4), 045003. https://doi.org/10.1088/1361-665X/aa5bd2.
(64) Agrawal, A. K.; Bhalla, R. Advances in the Production of Poly(Lactic Acid) Fibers. A Review. *Journal of Macromolecular Science, Part C* **2003**, *43* (4), 479–503. https://doi.org/10.1081/MC-120025975.
(65) Goessi, M.; Tervoort, T.; Smith, P. Melt-Spun Poly(Tetrafluoroethylene) Fibers. *J Mater Sci* **2007**, *42* (19), 7983–7990. https://doi.org/10.1007/s10853-006-1266-2.
(66) Edie, D. D.; Dunham, M. G. Melt Spinning Pitch-Based Carbon Fibers. *Carbon* **1989**, *27* (5), 647–655. https://doi.org/10.1016/0008-6223(89)90198-X.
(67) Strock, H. B.; Pascucci, M. R.; Parish, M. V.; Bent, A. A.; Shrout, T. R. Active PZT Fibers: A Commercial Production Process. In *Smart Structures and Materials 1999: Smart Materials Technologies*; International Society for Optics and Photonics, 1999; Vol. 3675, pp 22–31. https://doi.org/10.1117/12.352799.
(68) Ceramic Microfibers http://ceranova.com/products/ceramic-microfibers/ (accessed 2021 -02 -12).
(69) Kornmann, X.; Huber, C. Microstructure and Mechanical Properties of PZT Fibres. *Journal of the European Ceramic Society* **2004**, *24* (7), 1987–1991. https://doi.org/10.1016/S0955-2219(03)00364-9.
(70) Bowen, C. R.; Stevens, R.; Nelson, L. J.; Dent, A. C.; Dolman, G.; Su, B.; Button, T. W.; Cain, M. G.; Stewart, M. Manufacture and Characterization of High Activity Piezoelectric Fibres. *Smart Mater. Struct.* **2006**, *15* (2), 295–301. https://doi.org/10.1088/0964-1726/15/2/008.
(71) French, J. D.; Weitz, G. E.; Luke, J. E.; Cass, R. B.; Jadidian, B.; Bhargava, P.; Safari, A. Production of Continuous Piezoelectric Ceramic Fibers for Smart Materials and Active Control Devices. In *Smart Structures and Materials 1997: Industrial and Commercial Applications of Smart Structures Technologies*; International Society for Optics and Photonics, 1997; Vol. 3044, pp 406–412. https://doi.org/10.1117/12.274684.

(72) Mohammadi, F.; Khan, A.; Cass, R. B. Power Generation from Piezoelectric Lead Zirconate Titanate Fiber Composites. *MRS Online Proceedings Library* **2011**, *736* (1), 55. https://doi.org/10.1557/PROC-736-D5.5.
(73) Perepelkin, K. E. Lyocell Fibres Based on Direct Dissolution of Cellulose in N-Methylmorpholine N-Oxide: Development and Prospects. *Fibre Chem* **2007**, *39* (2), 163–172. https://doi.org/10.1007/s10692-007-0032-9.
(74) Smart Material PZT Fiber https://www.smart-material.com/PZTFiber-product-mainV2.html (accessed 2021 -08 -24).
(75) Selvaraj, U.; Prasadarao, A. V.; Komarneni, S.; Brooks, K.; Kurtz, S. Sol-Gel Processing of PbTiO3 and Pb(Zr0.52Ti0.48)O3 Fibers. *Journal of Materials Research* **1992**, *7* (4), 992–996. https://doi.org/10.1557/JMR.1992.0992.
(76) Qiu, J.; Tani, J.; Kobayashi, Y.; Um, T. Y.; Takahashi, H. Fabrication of Piezoelectric Ceramic Fibers by Extrusion of Pb(Zr, Ti)O3powder and Pb(Zr, Ti)O3sol Mixture. *Smart Mater. Struct.* **2003**, *12* (3), 331–337. https://doi.org/10.1088/0964-1726/12/3/303.
(77) Qiu, J.; Tani, J.; Yanada, N.; Kobayashi, Y.; Takahashi, H. Fabrication of Pb(Nb,Ni)O3-Pb(Zr,Ti)O3 Piezoelectric Ceramic Fibers by Extrusion of a Sol-Powder Mixture. *Journal of Intelligent Material Systems and Structures* **2004**, *15* (8), 643–653. https://doi.org/10.1177/1045389X04043949.
(78) Xiong, Z. X.; Pan, J.; Hu, P.; Xue, H.; Qiu, H.; Chen, L. F. Preparation and Properties of BaTiO3 Ceramic Fibers for Ferroelectric Applications. *Ferroelectrics* **2014**, *466* (1), 29–35. https://doi.org/10.1080/00150193.2014.894851.
(79) Yoshkawa, S.; Selvaraj, U.; Moses, P.; Jiang, Q.; Shrout, T. Pb(Zr,Ti)O3 [PZT] Fibers–Fabrication and Properties. *Ferroelectrics* **1994**, *154* (1), 325–330. https://doi.org/10.1080/00150199408017307.
(80) Meyer, R.; Shrout, T.; Yoshikawa, S. Lead Zirconate Titanate Fine Fibers Derived from Alkoxide-Based Sol-Gel Technology. *Journal of the American Ceramic Society* **1998**, *81* (4), 861–868. https://doi.org/10.1111/j.1151-2916.1998.tb02420.x.
(81) Dent, A. C.; Nelson, L. J.; Bowen, C. R.; Stevens, R.; Cain, M.; Stewart, M. Characterisation and Properties of Fine Scale PZT Fibres. *Journal of the European Ceramic Society* **2005**, *25* (12), 2387–2391. https://doi.org/10.1016/j.jeurceramsoc.2005.03.067.
(82) Safaei, M.; Sodano, H. A.; Anton, S. R. A Review of Energy Harvesting Using Piezoelectric Materials: State-of-the-Art a Decade Later (2008–2018). *Smart Mater. Struct.* **2019**, *28* (11), 113001. https://doi.org/10.1088/1361-665X/ab36e4.
(83) Tuloup, C.; Harizi, W.; Aboura, Z.; Meyer, Y.; Khellil, K.; Lachat, R. On the Manufacturing, Integration, and Wiring Techniques of in Situ Piezoelectric Devices for the Manufacturing and Structural Health Monitoring of Polymer–Matrix Composites: A Literature Review. *Journal of Intelligent Material Systems and Structures* **2019**, *30* (16), 2351–2381. https://doi.org/10.1177/1045389X19861782.
(84) Annamdas, V. G.; Radhika, M. A. Electromechanical Impedance of Piezoelectric Transducers for Monitoring Metallic and Non-Metallic Structures: A Review of Wired, Wireless and Energy-Harvesting Methods. *Journal of Intelligent Material Systems and Structures* **2013**, *24* (9), 1021–1042. https://doi.org/10.1177/1045389X13481254.
(85) Nelson, L. J. Smart Piezoelectric Fibre Composites. *Materials Science and Technology* **2002**, *18* (11), 1245–1256. https://doi.org/10.1179/026708302225007448.
(86) Wilkie, W. K.; Bryant, R. G.; High, J. W.; Fox, R. L.; Hellbaum, R. F.; Jr, A. J.; Little, B. D.; Mirick, P. H. Low-Cost Piezocomposite Actuator for Structural Control Applications. In *Smart Structures and Materials 2000: Industrial and Commercial*

Applications of Smart Structures Technologies; International Society for Optics and Photonics, 2000; Vol. 3991, pp 323–334. https://doi.org/10.1117/12.388175.

(87) Nelson, L.; Bowen, C.; Stevens, R.; Cain, M.; Stewart, M. Modeling and Measurement of Piezoelectric Fibers and Interdigitated Electrodes for the Optimization of Piezofibre Composites. In *Smart Structures and Materials 2003: Active Materials: Behavior and Mechanics*; International Society for Optics and Photonics, 2003; Vol. 5053, pp 556–567. https://doi.org/10.1117/12.484738.

(88) Smith, W. A. Modeling 1-3 Composite Piezoelectrics: Hydrostatic Response. *IEEE Transactions on Ultrasonics, Ferroelectrics, and Frequency Control* **1993**, *40* (1), 41–49. https://doi.org/10.1109/58.184997.

(89) Nelson, L. J.; Bowen, C. R. Determination of the Piezoelectric Properties of Fine Scale PZT Fibres. *Key Engineering Materials* **2001**, *206–213*, 1509–1512. https://doi.org/10.4028/www.scientific.net/KEM.206-213.1509.

(90) Watzka, W.; Seifert, S.; Scholz, H.; Sporn, D.; Schonecker, A.; Seffner, L. Dielectric and Ferroelectric Properties of 1-3 Composites Containing Thin PZT-Fibers. In *ISAF '96. Proceedings of the Tenth IEEE International Symposium on Applications of Ferroelectrics*; 1996; Vol. 2, pp 569–572. https://doi.org/10.1109/ISAF.1996.598042.

(91) Steinhausen, R.; Hauke, T.; Beige, H.; Watzka, W.; Lange, U.; Sporn, D.; Gebhardt, S.; Schönecker, A. Properties of Fine Scale Piezoelectric PZT Fibers with Different Zr Content. *Journal of the European Ceramic Society* **2001**, *21* (10), 1459–1462. https://doi.org/10.1016/S0955-2219(01)00041-3.

(92) Kozielski, L.; Clemens, F.; Lusiola, T.; Pilch, M. Uniaxial Extrusion as an Enhancement Method of Piezoelectric Properties of Ceramic Micro Fibers. *Journal of Alloys and Compounds* **2016**, *687*, 604–610. https://doi.org/10.1016/j.jallcom.2016.06.050.

(93) Bortolani, F.; del Campo, A.; Fernandez, J. F.; Clemens, F.; Rubio-Marcos, F. High Strain in (K,Na)NbO3-Based Lead-Free Piezoelectric Fibers. *Chem. Mater.* **2014**, *26* (12), 3838–3848. https://doi.org/10.1021/cm501538x.

(94) Gao, J.; Xue, D.; Liu, W.; Zhou, C.; Ren, X. Recent Progress on BaTiO3-Based Piezoelectric Ceramics for Actuator Applications. *Actuators* **2017**, *6* (3), 24. https://doi.org/10.3390/act6030024.

(95) Brei, D.; Cannon, B. J. Piezoceramic Hollow Fiber Active Composites. *Composites Science and Technology* **2004**, *64* (2), 245–261. https://doi.org/10.1016/S0266-3538(03)00259-8.

(96) Lin, Y.; Sodano, H. A. Concept and Model of a Piezoelectric Structural Fiber for Multifunctional Composites. *Composites Science and Technology* **2008**, *68* (7), 1911–1918. https://doi.org/10.1016/j.compscitech.2007.12.017.

(97) Danko, G. A.; Popovich, D.; Dogan, F. Piezoelectric Fibers Produced by the Fibrous Monolith Technique. In *Proceedings of the 21st Annual Conference on Composites, Advanced Ceramics, Materials, and Structures—A: Ceramic Engineering and Science Proceedings*; John Wiley & Sons, Ltd, 1997; pp 87–94. https://doi.org/10.1002/9780470294437.ch9.

(98) Qiu, J.; Tani, J.; Yamada, N.; Takahashi, H. Fabrication of Piezoelectric Fibers with Metal Core. In *Smart Structures and Materials 2003: Active Materials: Behavior and Mechanics*; International Society for Optics and Photonics, 2003; Vol. 5053, pp 475–483. https://doi.org/10.1117/12.484355.

(99) Hajjaji, A.; Benayad, A.; Sebald, G.; Pruvost, S.; Guiffard, B.; Qiu, J.; Guyomar, D. Synthesis and Characterization of 0.65Pb(Mg1/3Nb2/3)O3–0.35PbTiO3 Fibers with Pt Core. *Materials Research Bulletin* **2008**, *43* (3), 493–501. https://doi.org/10.1016/j.materresbull.2007.11.020.

(100) Yoon, C.-B.; Jun, S.-H.; Lee, S.-M.; Kim, H.-E.; Lee, K.-W. Piezoelectric Fibers with Uniform Internal Electrode by Co-Extrusion Process. *Journal of the American Ceramic Society* **2006**, *89* (4), 1333–1336. https://doi.org/10.1111/j.1551-2916.2005.00895.x.
(101) Sebald, G.; Qiu, J.; Guyomar, D.; Hoshi, D. Modeling and Characterization of Piezoelectric Fibers with Metal Core. *Jpn. J. Appl. Phys.* **2005**, *44* (8R), 6156. https://doi.org/10.1143/JJAP.44.6156.
(102) Bowland, C.; Zhou, Z.; Sodano, H. A. Multifunctional Barium Titanate Coated Carbon Fibers. *Advanced Functional Materials* **2014**, *24* (40), 6303–6308. https://doi.org/10.1002/adfm.201401417.
(103) Sato, H.; Shimojo, Y.; Sekiya, T. Development of the Piezoelectric Fiber and Application for the Smart Board. In *Smart Materials, Structures, and Systems*; International Society for Optics and Photonics: Bangalore, India, 2003; Vol. 5062, pp 292–296. https://doi.org/10.1117/12.514404.
(104) Bowland, C. C.; Sodano, H. A. Hydrothermal Synthesis of Tetragonal Phase BaTiO3 on Carbon Fiber with Enhanced Electromechanical Coupling. *J Mater Sci* **2017**, *52* (13), 7893–7906. https://doi.org/10.1007/s10853-017-0994-9.
(105) Newnham, R. E. Piezoelectricity. In *Properties of Materials: Anisotropy, Symmetry, Structure*; Oxford University Press, 2004; pp 87–100. https://doi.org/10.1093/oso/9780198520757.003.0014.
(106) Ferrari, B.; Moreno, R. EPD Kinetics: A Review. *Journal of the European Ceramic Society* **2010**, *30* (5), 1069–1078. https://doi.org/10.1016/j.jeurceramsoc.2009.08.022.
(107) Boccaccini, A. R.; Biest, O. van der; Talbot, J. B.; Division, E. S. E.; Foundation (U.S.), E. *Electrophoretic Deposition, Fundamentals and Applications: Proceedings of the International Symposium*; The Electrochemical Society, 2002.
(108) Besra, L.; Liu, M. A Review on Fundamentals and Applications of Electrophoretic Deposition (EPD). *Progress in Materials Science* **2007**, *52* (1), 1–61. https://doi.org/10.1016/j.pmatsci.2006.07.001.
(109) Sarkar, P.; De, D.; Rho, H. Synthesis and Microstructural Manipulation of Ceramics by Electrophoretic Deposition. *Journal of Materials Science* **2004**, *39* (3), 819–823. https://doi.org/10.1023/B:JMSC.0000012909.46419.0e.
(110) Boccaccini, A. R.; Zhitomirsky, I. Application of Electrophoretic and Electrolytic Deposition Techniques in Ceramics Processing. *Current Opinion in Solid State and Materials Science* **2002**, *6* (3), 251–260. https://doi.org/10.1016/S1359-0286(02)00080-3.
(111) Therese, G. H. A.; Kamath, P. V. Electrochemical Synthesis of Metal Oxides and Hydroxides. *Chem. Mater.* **2000**, *12* (5), 1195–1204. https://doi.org/10.1021/cm990447a.
(112) Lin, Y.; Shaffer, J. W.; Sodano, H. A. Electrolytic Deposition of PZT on Carbon Fibers for Fabricating Multifunctional Composites. *Smart Mater. Struct.* **2010**, *19* (12), 124004. https://doi.org/10.1088/0964-1726/19/12/124004.
(113) Louh, R.-F.; Hsu, Y.-H. Fabrication of Barium Titanate Ferroelectric Layers by Electrophoretic Deposition Technique. *Materials Chemistry and Physics* **2003**, *79* (2), 226–229. https://doi.org/10.1016/S0254-0584(02)00264-X.
(114) Kim, J.-W.; Heinrich, J. G. Influence of Processing Parameters on Microstructure and Ferroelectric Properties of PZT-Coated SiC Fibers. *Journal of the European Ceramic Society* **2005**, *25* (9), 1637–1645. https://doi.org/10.1016/j.jeurceramsoc.2004.05.011.
(115) Lin, Y.; Sodano, H. A. Fabrication and Electromechanical Characterization of a Piezoelectric Structural Fiber for Multifunctional Composites. *Advanced Functional Materials* **2009**, *19* (4), 592–598. https://doi.org/10.1002/adfm.200800859.

(116) Zhitomirsky, I. Electrophoretic and Electrolytic Deposition of Ceramic Coatings on Carbon Fibers. *Journal of the European Ceramic Society* **1998**, *18* (7), 849–856. https://doi.org/10.1016/S0955-2219(97)00213-6.
(117) Zhitomirsky, I. Cathodic Electrodeposition of Ceramic and Organoceramic Materials. Fundamental Aspects. *Advances in Colloid and Interface Science* **2002**, *97* (1), 279–317. https://doi.org/10.1016/S0001-8686(01)00068-9.
(118) Qin, Y.; Wang, X.; Wang, Z. L. Microfibre–Nanowire Hybrid Structure for Energy Scavenging. *Nature* **2008**, *451* (7180), 809–813. https://doi.org/10.1038/nature06601.
(119) Goel, S.; Kumar, B. A Review on Piezo-/Ferro-Electric Properties of Morphologically Diverse ZnO Nanostructures. *Journal of Alloys and Compounds* **2020**, *816*, 152491. https://doi.org/10.1016/j.jallcom.2019.152491.
(120) H. Malakooti, M.; A. Patterson, B.; Hwang, H.-S.; A. Sodano, H. ZnO Nanowire Interfaces for High Strength Multifunctional Composites with Embedded Energy Harvesting. *Energy & Environmental Science* **2016**, *9* (2), 634–643. https://doi.org/10.1039/C5EE03181H.
(121) Groo, L.; Inman, D. J.; Sodano, H. A. In Situ Damage Detection for Fiber-Reinforced Composites Using Integrated Zinc Oxide Nanowires. *Advanced Functional Materials* **2018**, *28* (35), 1802846. https://doi.org/10.1002/adfm.201802846.
(122) Mathur, S. C.; Scheinbeim, J. I.; Newman, B. A. Piezoelectric Properties and Ferroelectric Hysteresis Effects in Uniaxially Stretched Nylon-11 Films. *Journal of Applied Physics* **1984**, *56* (9), 2419–2425. https://doi.org/10.1063/1.334294.
(123) Harrison, J. S.; Ounaies, Z. Piezoelectric Polymers. In *Encyclopedia of Polymer Science and Technology*; American Cancer Society, 2002. https://doi.org/10.1002/0471440264.pst427.
(124) Dohany, J. E. Fluorine-Containing Polymers, Poly(Vinylidene Fluoride). In *Kirk-Othmer Encyclopedia of Chemical Technology*; American Cancer Society, 2000. https://doi.org/10.1002/0471238961.1615122504150801.a01.
(125) Broadhurst, M. G.; Davis, G. T. Physical Basis for Piezoelectricity in PVDF. *Ferroelectrics* **1984**, *60* (1), 3–13. https://doi.org/10.1080/00150198408017504.
(126) Lovinger, A. J. Poly(Vinylidene Fluoride). In *Developments in Crystalline Polymers—1*; Bassett, D. C., Ed.; The Developments Series; Springer Netherlands: Dordrecht, 1982; pp 195–273. https://doi.org/10.1007/978-94-009-7343-5_5.
(127) Newman, B. A.; Yoon, C. H.; Pae, K. D.; Scheinbeim, J. I. Piezoelectric Activity and Field-induced Crystal Structure Transitions in Poled Poly(Vinylidene Fluoride) Films. *Journal of Applied Physics* **1979**, *50* (10), 6095–6100. https://doi.org/10.1063/1.325778.
(128) Sessler, G. M. Piezoelectricity in Polyvinylidenefluoride. *The Journal of the Acoustical Society of America* **1981**, *70* (6), 1596–1608. https://doi.org/10.1121/1.387225.
(129) Bystrov, V. S.; Paramonova, E. V.; Bdikin, I. K.; Bystrova, A. V.; Pullar, R. C.; Kholkin, A. L. Molecular Modeling of the Piezoelectric Effect in the Ferroelectric Polymer Poly(Vinylidene Fluoride) (PVDF). *J Mol Model* **2013**, *19* (9), 3591–3602. https://doi.org/10.1007/s00894-013-1891-z.
(130) Wada, Y.; Hayakawa, R. A Model Theory of Piezo- and Pyroelectricity of Poly(Vinylidene Fluoride) Electret. *Ferroelectrics* **1981**, *32* (1), 115–118. https://doi.org/10.1080/00150198108238681.
(131) Furukawa, T.; Wen, J. X.; Suzuki, K.; Takashina, Y.; Date, M. Piezoelectricity and Pyroelectricity in Vinylidene Fluoride/Trifluoroethylene Copolymers. *Journal of Applied Physics* **1984**, *56* (3), 829–834. https://doi.org/10.1063/1.334016.

(132) Katsouras, I.; Asadi, K.; Li, M.; van Driel, T. B.; Kjær, K. S.; Zhao, D.; Lenz, T.; Gu, Y.; Blom, P. W. M.; Damjanovic, D.; Nielsen, M. M.; de Leeuw, D. M. The Negative Piezoelectric Effect of the Ferroelectric Polymer Poly(Vinylidene Fluoride). *Nature Mater* **2016**, *15* (1), 78–84. https://doi.org/10.1038/nmat4423.

(133) Egusa, S.; Wang, Z.; Chocat, N.; Ruff, Z. M.; Stolyarov, A. M.; Shemuly, D.; Sorin, F.; Rakich, P. T.; Joannopoulos, J. D.; Fink, Y. Multimaterial Piezoelectric Fibres. *Nature Mater* **2010**, *9* (8), 643–648. https://doi.org/10.1038/nmat2792.

(134) Lu, X.; Qu, H.; Skorobogatiy, M. Piezoelectric Micro- and Nanostructured Fibers Fabricated from Thermoplastic Nanocomposites Using a Fiber Drawing Technique: Comparative Study and Potential Applications. *ACS Nano* **2017**, *11* (2), 2103–2114. https://doi.org/10.1021/acsnano.6b08290.

(135) Lund, A.; Hagström, B. Melt Spinning of Poly(Vinylidene Fluoride) Fibers and the Influence of Spinning Parameters on β-Phase Crystallinity. *Journal of Applied Polymer Science* **2010**, *116* (5), 2685–2693. https://doi.org/10.1002/app.31789.

(136) Panda, P. K.; Tambe, S. R.; Thite, A. G. Zinc Oxide Nanorod as Effective Reinforcing Material for Enhancing β Phase Crystal in Poly(Vinylidene Fluoride) Filaments. *Journal of Composite Materials* **2020**, *54* (25), 3833–3839. https://doi.org/10.1177/0021998320921548.

(137) Chapron, D.; Rault, F.; Talbourdet, A.; Lemort, G.; Cochrane, C.; Bourson, P.; Devaux, E.; Campagne, C. In-Situ Raman Monitoring of the Poly(Vinylidene Fluoride) Crystalline Structure during a Melt-Spinning Process. *Journal of Raman Spectroscopy* **2021**, *52* (5), 1073–1079. https://doi.org/10.1002/jrs.6081.

(138) Cakmak, M.; Teitge, A.; Zachmann, H. G.; White, J. L. On-Line Small-Angle and Wide-Angle x-Ray Scattering Studies on Melt-Spinning Poly(Vinylidene Fluoride) Tape Using Synchrotron Radiation. *Journal of Polymer Science Part B: Polymer Physics* **1993**, *31* (3), 371–381. https://doi.org/10.1002/polb.1993.090310316.

(139) Martins, P.; Lopes, A. C.; Lanceros-Mendez, S. Electroactive Phases of Poly(Vinylidene Fluoride): Determination, Processing and Applications. *Progress in Polymer Science* **2014**, *39* (4), 683–706. https://doi.org/10.1016/j.progpolymsci.2013.07.006.

(140) Sukumaran, S.; Chatbouri, S.; Rouxel, D.; Tisserand, E.; Thiebaud, F.; Ben Zineb, T. Recent Advances in Flexible PVDF Based Piezoelectric Polymer Devices for Energy Harvesting Applications. *Journal of Intelligent Material Systems and Structures* **2021**, *32* (7), 746–780. https://doi.org/10.1177/1045389X20966058.

(141) Talbourdet, A.; Rault, F.; Cayla, A.; Cochrane, C.; Devaux, E.; Gonthier, A.; Lemort, G.; Campagne, C. Development of Mono-Component and Tri-Component Fibres 100% Polymer Based Piezoelectric PVDF to Harvest Energy. *IOP Conf. Ser.: Mater. Sci. Eng.* **2017**, *254*, 072026. https://doi.org/10.1088/1757-899X/254/7/072026.

(142) Yang, J.; Chen, Q.; Chen, F.; Zhang, Q.; Wang, K.; Fu, Q. Realizing the Full Nanofiller Enhancement in Melt-Spun Fibers of Poly(Vinylidene Fluoride)/Carbon Nanotube Composites. *Nanotechnology* **2011**, *22* (35), 355707. https://doi.org/10.1088/0957-4484/22/35/355707.

(143) Soin, N.; H. Shah, T.; C. Anand, S.; Geng, J.; Pornwannachai, W.; Mandal, P.; Reid, D.; Sharma, S.; L. Hadimani, R.; Vatansever Bayramol, D.; Siores, E. Novel "3-D Spacer" All Fibre Piezoelectric Textiles for Energy Harvesting Applications. *Energy & Environmental Science* **2014**, *7* (5), 1670–1679. https://doi.org/10.1039/C3EE43987A.

(144) Guo, Z.; Nilsson, E.; Rigdahl, M.; Hagström, B. Melt Spinning of PVDF Fibers with Enhanced β Phase Structure. *Journal of Applied Polymer Science* **2013**, *130* (4), 2603–2609. https://doi.org/10.1002/app.39484.

(145) Boudriaux, M.; Rault, F.; Cochrane, C.; Lemort, G.; Campagne, C.; Devaux, E.; Courtois, C. Crystalline Forms of PVDF Fiber Filled with Clay Components along Processing Steps. *Journal of Applied Polymer Science* **2016**, *133* (14). https://doi.org/10.1002/app.43244.
(146) Bairagi, S.; Wazed Ali, S. A Unique Piezoelectric Nanogenerator Composed of Melt-Spun PVDF/KNN Nanorods Based Nanocomposite Fibre. *European Polymer Journal* **2019**. https://doi.org/10.1016/j.eurpolymj.2019.04.043.
(147) Yuan, J.-K.; Yao, S.-H.; Dang, Z.-M.; Sylvestre, A.; Genestoux, M.; Bai1, J. Giant Dielectric Permittivity Nanocomposites: Realizing True Potential of Pristine Carbon Nanotubes in Polyvinylidene Fluoride Matrix through an Enhanced Interfacial Interaction. *J. Phys. Chem. C* **2011**, *115* (13), 5515–5521. https://doi.org/10.1021/jp1117163.
(148) Matsuyama, H.; Rajabzadeh, S.; Karkhanechi, H.; Jeon, S. 1.7 PVDF Hollow Fibers Membranes. In *Comprehensive Membrane Science and Engineering*; Elsevier, 2017; pp 137–189. https://doi.org/10.1016/B978-0-12-409547-2.12244-9.
(149) Hwang, S. K.; Kwon, O. M.; Hwang, H. Y. Adhesion Characteristics of Piezoelectric Polymer Fibers for Multifunctioal Composites; Venice, Italy, 2012.
(150) Jeong, K.; Kim, D. H.; Chung, Y. S.; Hwang, S. K.; Hwang, H. Y.; Kim, S. S. Effect of Processing Parameters of the Continuous Wet Spinning System on the Crystal Phase of PVDF Fibers. *Journal of Applied Polymer Science* **2018**, *135* (3), 45712. https://doi.org/10.1002/app.45712.
(151) Tascan, M.; Nohut, S. Effects of Process Parameters on the Properties of Wet-Spun Solid PVDF Fibers. *Textile Research Journal* **2014**, *84* (20), 2214–2225. https://doi.org/10.1177/0040517514535869.
(152) Broadhust, M. G.; Davis, G. T. Piezo- and Pyroelectric Properties. In *Electrets*; Sessler, G. ., Ed.; Topics in Applied Physics; G. M. Sessler, 1980; Vol. 33, pp 285–315.
(153) Lund, A.; Hagström, B. Melt Spinning of β-Phase Poly(Vinylidene Fluoride) Yarns with and without a Conductive Core. *Journal of Applied Polymer Science* **2011**, *120* (2), 1080–1089. https://doi.org/10.1002/app.33239.
(154) Glauß, B.; Steinmann, W.; Walter, S.; Beckers, M.; Seide, G.; Gries, T.; Roth, G. Spinnability and Characteristics of Polyvinylidene Fluoride (PVDF)-Based Bicomponent Fibers with a Carbon Nanotube (CNT) Modified Polypropylene Core for Piezoelectric Applications. *Materials* **2013**, *6* (7), 2642–2661. https://doi.org/10.3390/ma6072642.
(155) Glauß, B.; Jux, M.; Walter, S.; Kubicka, M.; Seide, G.; Wierach, P.; Gries, T.; Roth, G. Poling Effects in Melt-Spun PVDF Bicomponent Fibres. *Key Engineering Materials* **2015**, *644*, 110–114. https://doi.org/10.4028/www.scientific.net/KEM.644.110.
(156) Kechiche, M. B.; Bauer, F.; Harzallah, O.; Drean, J.-Y. Development of Piezoelectric Coaxial Filament Sensors P(VDF-TrFE)/Copper for Textile Structure Instrumentation. *Sensors and Actuators A: Physical* **2013**, *204*, 122–130. https://doi.org/10.1016/j.sna.2013.10.007.
(157) Grujicic, M.; Sellappan, V.; Omar, M. A.; Seyr, N.; Obieglo, A.; Erdmann, M.; Holzleitner, J. An Overview of the Polymer-to-Metal Direct-Adhesion Hybrid Technologies for Load-Bearing Automotive Components. *Journal of Materials Processing Technology* **2008**, *197* (1), 363–373. https://doi.org/10.1016/j.jmatprotec.2007.06.058.

(158) Liu, W.; Chen, R.; Ruan, X.; Fu, X. Polymeric Piezoelectric Fiber with Metal Core Produced by Electrowetting-Aided Dry Spinning Method. *Journal of Applied Polymer Science* **2016**, *133* (39). https://doi.org/10.1002/app.43968.
(159) Yee, W. A.; Kotaki, M.; Liu, Y.; Lu, X. Morphology, Polymorphism Behavior and Molecular Orientation of Electrospun Poly(Vinylidene Fluoride) Fibers. *Polymer* **2007**, *48* (2), 512–521. https://doi.org/10.1016/j.polymer.2006.11.036.
(160) Defebvin, J.; Barrau, S.; Lyskawa, J.; Woisel, P.; Lefebvre, J.-M. Influence of Nitrodopamine-Functionalized Barium Titanate Content on the Piezoelectric Response of Poly(Vinylidene Fluoride) Based Polymer-Ceramic Composites. *Composites Science and Technology* **2017**, *147*, 16–21. https://doi.org/10.1016/j.compscitech.2017.05.001.
(161) Yamada, T.; Ueda, T.; Kitayama, T. Piezoelectricity of a High-content Lead Zirconate Titanate/Polymer Composite. *Journal of Applied Physics* **1982**, *53* (6), 4328–4332. https://doi.org/10.1063/1.331211.
(162) David, C.; Capsal, J.-F.; Laffont, L.; Dantras, E.; Lacabanne, C. Piezoelectric Properties of Polyamide 11/NaNbO3nanowire Composites. *J. Phys. D: Appl. Phys.* **2012**, *45* (41), 415305. https://doi.org/10.1088/0022-3727/45/41/415305.
(163) Qi, F.; Chen, N.; Wang, Q. Preparation of PA11/BaTiO3 Nanocomposite Powders with Improved Processability, Dielectric and Piezoelectric Properties for Use in Selective Laser Sintering. *Materials & Design* **2017**, *131*, 135–143. https://doi.org/10.1016/j.matdes.2017.06.012.
(164) Carponcin, D.; Dantras, E.; Laffont, L.; Dandurand, J.; Aridon, G.; Levallois, F.; Cadiergues, L.; Lacabanne, C. Integrated Piezoelectric Function in a High Thermostable Thermoplastic PZT/PEEK Composite. *Journal of Non-Crystalline Solids* **2014**, *388*, 32–36. https://doi.org/10.1016/j.jnoncrysol.2014.01.020.
(165) Landauer, R. The Electrical Resistance of Binary Metallic Mixtures. *Journal of Applied Physics* **1952**, *23* (7), 779–784. https://doi.org/10.1063/1.1702301.
(166) Tuff, W.; Manghera, P.; Tilghman, J.; Van Fossen, E.; Chowdhury, S.; Ahmed, S.; Banerjee, S. BaTiO3–Epoxy–ZnO-Based Multifunctional Composites: Variation in Electron Transport Properties Due to the Interaction of ZnO Nanoparticles with the Composite Microstructure. *Journal of Elec Materi* **2019**, *48* (8), 4987–4996. https://doi.org/10.1007/s11664-019-07292-6.
(167) Arbatti, M.; Shan, X.; Cheng, Z. Ceramic-Polymer Composites with High Dielectric Constant. *Advanced Materials* **2007**, *19* (10), 1369–1372. https://doi.org/10.1002/adma.200601996.
(168) Li, R.; Guo, Q.; Shi, Z.; Pei, J. Effects of Conductive Carbon Black on PZT/PVDF Composites. *Ferroelectrics* **2018**, *526* (1), 176–186. https://doi.org/10.1080/00150193.2018.1456308.
(169) Maxwell, K. S.; Whitcomb, J. D.; Ounaies, Z.; Barhoumi, A. Finite Element Analysis of a Three-Phase Piezoelectric Nanocomposite. *Journal of Intelligent Material Systems and Structures* **2010**, *21* (11), 1073–1084. https://doi.org/10.1177/1045389X10375484.
(170) Carponcin, D.; Dantras, E.; Dandurand, J.; Aridon, G.; Levallois, F.; Cadiergues, L.; Lacabanne, C. Electrical and Piezoelectric Behavior of Polyamide/PZT/CNT Multifunctional Nanocomposites. *Advanced Engineering Materials* **2014**, *16* (8), 1018–1025. https://doi.org/10.1002/adem.201300519.
(171) Li, J.; Claude, J.; Norena-Franco, L. E.; Seok, S. I.; Wang, Q. Electrical Energy Storage in Ferroelectric Polymer Nanocomposites Containing Surface-Functionalized BaTiO3 Nanoparticles. *Chem. Mater.* **2008**, *20* (20), 6304–6306. https://doi.org/10.1021/cm8021648.

(172) Kim, P.; Doss, N. M.; Tillotson, J. P.; Hotchkiss, P. J.; Pan, M.-J.; Marder, S. R.; Li, J.; Calame, J. P.; Perry, J. W. High Energy Density Nanocomposites Based on Surface-Modified BaTiO3 and a Ferroelectric Polymer. *ACS Nano* **2009**, *3* (9), 2581–2592. https://doi.org/10.1021/nn9006412.
(173) Dai, Z.-H.; Han, J.-R.; Gao, Y.; Xu, J.; He, J.; Guo, B.-H. Increased Dielectric Permittivity of Poly(Vinylidene Fluoride-Co-Chlorotrifluoroethylene) Nanocomposites by Coating BaTiO3 with Functional Groups Owning High Bond Dipole Moment. *Colloids and Surfaces A: Physicochemical and Engineering Aspects* **2017**, *529*, 560–570. https://doi.org/10.1016/j.colsurfa.2017.05.065.
(174) Dai, Z.-H.; Li, T.; Gao, Y.; Xu, J.; Weng, Y.; He, J.; Guo, B.-H. Improved Dielectric and Energy Storage Properties of Poly(Vinyl Alcohol) Nanocomposites by Strengthening Interfacial Hydrogen-Bonding Interaction. *Colloids and Surfaces A: Physicochemical and Engineering Aspects* **2018**, *548*, 179–190. https://doi.org/10.1016/j.colsurfa.2018.03.056.
(175) Mayeen, A.; S, K. M.; Jayalakshmy, M. S.; Thomas, S.; Rouxel, D.; Philip, J.; Bhowmik, R. N.; Kalarikkal, N. Dopamine Functionalization of BaTiO3: An Effective Strategy for the Enhancement of Electrical, Magnetoelectric and Thermal Properties of BaTiO3-PVDF-TrFE Nanocomposites. *Dalton Trans.* **2018**, *47* (6), 2039–2051. https://doi.org/10.1039/C7DT03389C.
(176) Yang, D.; Kong, X.; Ni, Y.; Xu, Y.; Huang, S.; Shang, G.; Xue, H.; Guo, W.; Zhang, L. Enhancement of Dielectric Performance of Polymer Composites via Constructing BaTiO3–Poly(Dopamine)–Ag Nanoparticles through Mussel-Inspired Surface Functionalization. *ACS Omega* **2018**, *3*, 14087–14096. https://doi.org/10.1021/acsomega.8b02367.
(177) Luo, H.; Zhou, X.; Ellingford, C.; Zhang, Y.; Chen, S.; Zhou, K.; Zhang, D.; R. Bowen, C.; Wan, C. Interface Design for High Energy Density Polymer Nanocomposites. *Chemical Society Reviews* **2019**, *48* (16), 4424–4465. https://doi.org/10.1039/C9CS00043G.
(178) Ren, K.; Liu, Y.; Geng, X.; Hofmann, H. F.; Zhang, Q. M. Single Crystal PMN-PT/Epoxy 1-3 Composite for Energy-Harvesting Application. *IEEE Transactions on Ultrasonics, Ferroelectrics, and Frequency Control* **2006**, *53* (3), 631–638. https://doi.org/10.1109/TUFFC.2006.1610572.
(179) Nafari, A.; Sodano, H. A. Electromechanical Modeling and Experimental Verification of a Direct Write Nanocomposite. *Smart Mater. Struct.* **2019**, *28* (4), 045014. https://doi.org/10.1088/1361-665X/aadb6c.
(180) Andrews, C.; Lin, Y.; Sodano, H. A. The Effect of Particle Aspect Ratio on the Electroelastic Properties of Piezoelectric Nanocomposites. *Smart Mater. Struct.* **2010**, *19* (2), 025018. https://doi.org/10.1088/0964-1726/19/2/025018.
(181) Tang, H.; Lin, Y.; Andrews, C.; Sodano, H. A. Nanocomposites with Increased Energy Density through High Aspect Ratio PZT Nanowires. *Nanotechnology* **2010**, *22* (1), 015702. https://doi.org/10.1088/0957-4484/22/1/015702.
(182) Andrews, C.; Lin, Y.; Tang, H.; Sodano, H. A. Influence of Aspect Ratio on Effective Electromechanical Coupling of Nanocomposites with Lead Zirconate Titanate Nanowire Inclusion. *Journal of Intelligent Material Systems and Structures* **2011**, *22* (16), 1879–1886. https://doi.org/10.1177/1045389X11416025.
(183) Osoka, E. C.; Onukwuli, O. D. A Modified Halpin-Tsai Model for Estimating the Modulus of Natural Fiber Reinforced Composites. *(IJESI)* **2018**, *07* (05), 63–70.
(184) Oh, H. J.; Kim, D.-K.; Choi, Y. C.; Lim, S.-J.; Jeong, J. B.; Ko, J. H.; Hahm, W.-G.; Kim, S.-W.; Lee, Y.; Kim, H.; Yeang, B. J. Fabrication of Piezoelectric Poly(l -Lactic

Acid)/BaTiO 3 Fibre by the Melt-Spinning Process. *Scientific Reports* **2020**, *10* (1), 16339. https://doi.org/10.1038/s41598-020-73261-3.
(185) Mokhtari, F.; Spinks, G. M.; Fay, C.; Cheng, Z.; Raad, R.; Xi, J.; Foroughi, J. Wearable Electronic Textiles from Nanostructured Piezoelectric Fibers. *Advanced Materials Technologies* **2020**, *5* (4), 1900900. https://doi.org/10.1002/admt.201900900.
(186) Mercader, C.; Denis-Lutard, V.; Jestin, S.; Maugey, M.; Derré, A.; Zakri, C.; Poulin, P. Scalable Process for the Spinning of PVA-Carbon Nanotube Composite Fibers. *Journal of Applied Polymer Science* **2012**, *125* (SUPPL. 1), E191–E196. https://doi.org/10.1002/app.36308.
(187) Kinadjian, N.; Achard, M.-F.; Julián-López, B.; Maugey, M.; Poulin, P.; Prouzet, E.; Backov, R. ZnO/PVA Macroscopic Fibers Bearing Anisotropic Photonic Properties. *Advanced Functional Materials* **2012**, *22* (19), 3994–4003. https://doi.org/10.1002/adfm.201200360.
(188) Biette, L.; Carn, F.; Maugey, M.; Achard, M.-F.; Maquet, J.; Steunou, N.; Livage, J.; Serier, H.; Backov, R. Macroscopic Fibers of Oriented Vanadium Oxide Ribbons and Their Application as Highly Sensitive Alcohol Microsensors. *Advanced Materials* **2005**, *17* (24), 2970–2974. https://doi.org/10.1002/adma.200501368.
(189) Zhang, M.; Gao, T.; Wang, J.; Liao, J.; Qiu, Y.; Xue, H.; Shi, Z.; Xiong, Z.; Chen, L. Single BaTiO3 Nanowires-Polymer Fiber Based Nanogenerator. *Nano Energy* **2015**, *11*, 510–517. https://doi.org/10.1016/j.nanoen.2014.11.028.
(190) Lee, M.; Chen, C.-Y.; Wang, S.; Cha, S. N.; Park, Y. J.; Kim, J. M.; Chou, L.-J.; Wang, Z. L. A Hybrid Piezoelectric Structure for Wearable Nanogenerators. *Advanced Materials* **2012**, *24* (13), 1759–1764. https://doi.org/10.1002/adma.201200150.
(191) Arica, T. A.; Isık, T.; Guner, T.; Horzum, N.; Demir, M. M. Advances in Electrospun Fiber-Based Flexible Nanogenerators for Wearable Applications. *Macromolecular Materials and Engineering* **2021**, *306* (8), 2100143. https://doi.org/10.1002/mame.202100143.
(192) Esfahani, H.; Jose, R.; Ramakrishna, S. Electrospun Ceramic Nanofiber Mats Today: Synthesis, Properties, and Applications. *Materials* **2017**, *10* (11), 1238. https://doi.org/10.3390/ma10111238.
(193) Krajewski, A. S.; Magniez, K.; Helmer, R. J. N.; Schrank, V. Piezoelectric Force Response of Novel 2D Textile Based PVDF Sensors. *IEEE Sensors Journal* **2013**, *13* (12), 4743–4748. https://doi.org/10.1109/JSEN.2013.2274151.
(194) Tajitsu, Y. Development of Electric Control Catheter and Tweezers for Thrombosis Sample in Blood Vessels Using Piezoelectric Polymeric Fibers. *Polymers for Advanced Technologies* **2006**, *17* (11–12), 907–913. https://doi.org/10.1002/pat.817.
(195) Nilsson, E.; Lund, A.; Jonasson, C.; Johansson, C.; Hagström, B. Poling and Characterization of Piezoelectric Polymer Fibers for Use in Textile Sensors. *Sensors and Actuators A: Physical* **2013**, *201*, 477–486. https://doi.org/10.1016/j.sna.2013.08.011.
(196) Talbourdet, A.; Rault, F.; Lemort, G.; Cochrane, C.; Devaux, E.; Campagne, C. 3D Interlock Design 100% PVDF Piezoelectric to Improve Energy Harvesting. *Smart Mater. Struct.* **2018**, *27* (7), 075010. https://doi.org/10.1088/1361-665X/aab865.
(197) Zhang, M.; Gao, T.; Wang, J.; Liao, J.; Qiu, Y.; Yang, Q.; Xue, H.; Shi, Z.; Zhao, Y.; Xiong, Z.; Chen, L. A Hybrid Fibers Based Wearable Fabric Piezoelectric Nanogenerator for Energy Harvesting Application. *Nano Energy* **2015**, *13*, 298–305. https://doi.org/10.1016/j.nanoen.2015.02.034.

(198) Tajitsu, Y. Smart Piezoelectric Fabric and Its Application to Control of Humanoid Robot. *Ferroelectrics* **2016**, *499* (1), 36–46. https://doi.org/10.1080/00150193.2016.1171982.
(199) Tajitsu, Y. Sensing Complicated Motion of Human Body Using Piezoelectric Chiral Polymer Fiber. *Ferroelectrics* **2015**, *480* (1), 32–38. https://doi.org/10.1080/00150193.2015.1012410.
(200) Lund, A.; Rundqvist, K.; Nilsson, E.; Yu, L.; Hagström, B.; Müller, C. Energy Harvesting Textiles for a Rainy Day: Woven Piezoelectrics Based on Melt-Spun PVDF Microfibres with a Conducting Core. *npj Flexible Electronics* **2018**, *2* (1), 1–9. https://doi.org/10.1038/s41528-018-0022-4.
(201) Åkerfeldt, M.; Nilsson, E.; Gillgard, P.; Walkenström, P. Textile Piezoelectric Sensors – Melt Spun Bi-Component Poly(Vinylidene Fluoride) Fibres with Conductive Cores and Poly(3,4-Ethylene Dioxythiophene)-Poly(Styrene Sulfonate) Coating as the Outer Electrode. *Fashion and Textiles* **2014**, *1* (1), 13. https://doi.org/10.1186/s40691-014-0013-6.
(202) Åkerfeldt, M.; Lund, A.; Walkenström, P. Textile Sensing Glove with Piezoelectric PVDF Fibers and Printed Electrodes of PEDOT:PSS. *Textile Research Journal* **2015**, *85* (17), 1789–1799. https://doi.org/10.1177/0040517515578333.
(203) Gao, F.; Liu, G.; Chung, B. L.-H.; Chan, H. H.-T.; Liao, W.-H. Macro Fiber Composite-Based Energy Harvester for Human Knee. *Appl. Phys. Lett.* **2019**, *115* (3), 033901. https://doi.org/10.1063/1.5098962.
(204) Grzybek, D.; Micek, P. Piezoelectric Energy Harvesting Based on Macro Fiber Composite from a Rotating Shaft. *Phys. Scr.* **2019**, *94* (9), 095802. https://doi.org/10.1088/1402-4896/ab0d49.
(205) Liu, J.; Zuo, H.; Xia, W.; Luo, Y.; Yao, D.; Chen, Y.; Wang, K.; Li, Q. Wind Energy Harvesting Using Piezoelectric Macro Fiber Composites Based on Flutter Mode. *Microelectronic Engineering* **2020**, *231*, 111333. https://doi.org/10.1016/j.mee.2020.111333.
(206) Hu, D.; Lou, J.; Chen, T.; Yang, Y.; Xu, C.; Chen, H.; Cui, Y. Micro Thrust Measurement Experiment and Pressure Field Evolution of Bionic Robotic Fish with Harmonic Actuation of Macro Fiber Composites. *Mechanical Systems and Signal Processing* **2021**, *153*, 107538. https://doi.org/10.1016/j.ymssp.2020.107538.
(207) Lin, X.; Zhou, K.; Zhang, X.; Zhang, D. Development, Modeling and Application of Piezoelectric Fiber Composites. *Transactions of Nonferrous Metals Society of China* **2013**, *23* (1), 98–107. https://doi.org/10.1016/S1003-6326(13)62435-8.
(208) MacroFiberComposite™ https://www.smart-material.com/MFC-product-mainV2.html (accessed 2022 -03 -04).
(209) Sodano, H. A.; Park, G.; Inman, D. J. An Investigation into the Performance of Macro-Fiber Composites for Sensing and Structural Vibration Applications. *Mechanical Systems and Signal Processing* **2004**, *18* (3), 683–697. https://doi.org/10.1016/S0888-3270(03)00081-5.
(210) PRABAKAR, K.; MALLIKARJUN RAO, S. P. Acoustic Emission During Phase Transition in Soft PZT Ceramics Under an Applied Electric Field. *Ferroelectrics Letters Section* **2005**, *32* (5–6), 99–110. https://doi.org/10.1080/07315170500416579.
(211) Li, W.; Kong, Q.; Ho, S. C. M.; Lim, I.; Mo, Y. L.; Song, G. Feasibility Study of Using Smart Aggregates as Embedded Acoustic Emission Sensors for Health Monitoring of Concrete Structures. *Smart Mater. Struct.* **2016**, *25* (11), 115031. https://doi.org/10.1088/0964-1726/25/11/115031.

(212) Henslee, I. A.; Miller, D. A.; Tempero, T. Fatigue Life Characterization for Piezoelectric Macrofiber Composites. *Smart Mater. Struct.* **2012**, *21* (10), 105037. https://doi.org/10.1088/0964-1726/21/10/105037.
(213) Pandey, A.; Arockiarajan, A. Fatigue Study on the Actuation Performance of Macro Fiber Composite (MFC): Theoretical and Experimental Approach. *Smart Mater. Struct.* **2017**, *26* (3), 035018. https://doi.org/10.1088/1361-665X/aa59e9.
(214) Bowen, C. R.; Dent, A. C.; Nelson, L. J.; Stevens, R.; Cain, M. G.; Stewart, M. Failure and Volume Fraction Dependent Mechanical Properties of Composite Sensors and Actuators. *Proceedings of the Institution of Mechanical Engineers, Part C: Journal of Mechanical Engineering Science* **2006**, *220* (11), 1655–1663. https://doi.org/10.1243/09544062JMES255.
(215) Martinez, M.; Artemev, A. Finite Element Analysis of Broken Fiber Effects on the Performance of Active Fiber Composites. *Composite Structures* **2009**, *88* (3), 491–496. https://doi.org/10.1016/j.compstruct.2008.06.004.
(216) Karalekas, D.; Cugnoni, J.; Botsis, J. Monitoring of Process Induced Strains in a Single Fibre Composite Using FBG Sensor: A Methodological Study. *Composites Part A: Applied Science and Manufacturing* **2008**, *39* (7), 1118–1127. https://doi.org/10.1016/j.compositesa.2008.04.010.
(217) de Oliveira, R.; Ramos, C. A.; Marques, A. T. Health Monitoring of Composite Structures by Embedded FBG and Interferometric Fabry–Pérot Sensors. *Computers & Structures* **2008**, *86* (3), 340–346. https://doi.org/10.1016/j.compstruc.2007.01.040.
(218) Groo, L.; Steinke, K.; Inman, D. J.; Sodano, H. A. Vibration Damping Mechanism of Fiber-Reinforced Composites with Integrated Piezoelectric Nanowires. *ACS Appl. Mater. Interfaces* **2019**, *11* (50), 47373–47381. https://doi.org/10.1021/acsami.9b17029.
(219) Duffy, K. P.; Choi, B. B.; Provenza, A. J.; Min, J. B.; Kray, N. Active Piezoelectric Vibration Control of Subscale Composite Fan Blades. *Journal of Engineering for Gas Turbines and Power* **2012**, *135* (011601). https://doi.org/10.1115/1.4007720.
(220) Ray, M. C.; Pradhan, A. K. On the Use of Vertically Reinforced 1-3 Piezoelectric Composites for Hybrid Damping of Laminated Composite Plates. *Mechanics of Advanced Materials and Structures* **2007**, *14* (4), 245–261. https://doi.org/10.1080/15376490600795683.
(221) Sarangi, S. K.; Ray, M. C. Active Damping of Geometrically Nonlinear Vibrations of Doubly Curved Laminated Composite Shells. *Composite Structures* **2011**, *93* (12), 3216–3228. https://doi.org/10.1016/j.compstruct.2011.06.005.
(222) Zhang, H. Y.; Shen, Y. P. Vibration Suppression of Laminated Plates with 1–3 Piezoelectric Fiber-Reinforced Composite Layers Equipped with Interdigitated Electrodes. *Composite Structures* **2007**, *79* (2), 220–228. https://doi.org/10.1016/j.compstruct.2005.12.003.
(223) Williams, R. B.; Inman, D. J.; Wilkie, W. K. Nonlinear Response of the Macro Fiber Composite Actuator to Monotonically Increasing Excitation Voltage. *Journal of Intelligent Material Systems and Structures* **2006**, *17* (7), 601–608. https://doi.org/10.1177/1045389X06059501.
(224) Jemai, A.; Najar, F.; Chafra, M.; Ounaies, Z. Modeling and Parametric Analysis of a Unimorph Piezocomposite Energy Harvester with Interdigitated Electrodes. *Composite Structures* **2016**, *135*, 176–190. https://doi.org/10.1016/j.compstruct.2015.09.017.
(225) Khazaee, M.; Rezaniakolaie, A.; Rosendahl, L. A Broadband Macro-Fiber-Composite Piezoelectric Energy Harvester for Higher Energy Conversion from Practical

Wideband Vibrations. *Nano Energy* **2020**, *76*, 104978. https://doi.org/10.1016/j.nanoen.2020.104978.
(226) Ju, S.; Ji, C.-H. Impact-Based Piezoelectric Vibration Energy Harvester. *Applied Energy* **2018**, *214*, 139–151. https://doi.org/10.1016/j.apenergy.2018.01.076.